

# Starvation as the primary quenching mechanism in galaxies

James Trussler,<sup>1,2\*</sup> Roberto Maiolino,<sup>1,2</sup> Claudia Maraston,<sup>3</sup> Yingjie Peng,<sup>4</sup>  
Daniel Thomas,<sup>3</sup> Daniel Goddard<sup>3</sup> and Jianhui Lian<sup>3</sup>

<sup>1</sup>*Cavendish Laboratory, University of Cambridge, 19 J.J. Thomson Avenue, Cambridge, CB3 0HE, UK*

<sup>2</sup>*Kavli Institute for Cosmology, University of Cambridge, Madingley Road, Cambridge CB3 0HA, UK*

<sup>3</sup>*Institute of Cosmology and Gravitation, University of Portsmouth, Portsmouth PO1 3FX, UK*

<sup>4</sup>*Kavli Institute for Astronomy and Astrophysics, Peking University, Beijing 100871, China*

Accepted XXX. Received YYY; in original form ZZZ

## ABSTRACT

Star-forming galaxies can in principle be transformed into passive systems by a multitude of processes that quench star formation, such as the halting of gas accretion or the rapid removal of gas in AGN-driven outflows. However, it remains unclear which processes are the most significant, primary drivers of the SF-passive bimodality. We address this key issue in galaxy evolution by studying the chemical properties of 80,000 local galaxies in SDSS DR7. In order to distinguish between different quenching mechanisms, we analyse the systematic difference in mass-weighted stellar metallicity between star-forming, green valley and passive galaxies. Our analysis reveals that the star-forming progenitors of massive ( $M_* \sim 10^{11} M_\odot$ ) local passive galaxies quenched primarily through starvation over a time-scale of 2 Gyr, before any future star formation was abruptly halted by an ejective or heating mode. We find that outflows played a minor role in quenching the progenitors of massive galaxies, but were of increasing importance in quenching the progenitors of low-mass ( $M_* < 10^{10} M_\odot$ ) passive galaxies over a typical time-scale of 5 Gyr. Furthermore, our analysis reveals that local green valley galaxies have typically been quenching through starvation for 3.5 Gyr, indicating that galaxies in the local Universe quench more slowly than their counterparts at higher redshift. Finally, we find that the quenching of central galaxies is independent of the environment. In contrast, we find that environmental effects contributed to the starvation of low-mass satellite galaxies in very dense environments.

**Key words:** galaxies: evolution – galaxies: abundances– galaxies: star formation

## 1 INTRODUCTION

Galaxies in the local Universe exhibit a bimodality in many of their key properties, such as colour (e.g. [Strateva et al. 2001](#); [Blanton et al. 2003](#); [Baldry et al. 2004](#)), star formation rate (e.g. [Noeske et al. 2007](#); [Mcgee et al. 2011](#); [Wetzel et al. 2012](#)), stellar age (e.g. [Kauffmann et al. 2003](#); [Galazzi et al. 2008](#)) and morphology (e.g. [Wuyts et al. 2011](#); [van der Wel et al. 2014](#)). Galaxies are therefore broadly divided into two main classes: star-forming and passive. Star-forming galaxies typically have blue colours, young stellar populations and late-type morphologies. On the other hand, passive galaxies are not actively forming stars and typically have red colours, old stellar populations and early-type morphologies. Deeper observations have revealed evidence for galaxy bimodality up to  $z \sim 4$  (e.g. [Brammer et al. 2009](#); [Muzzin et al. 2013](#)), identifying a population of massive,

passive galaxies at high redshift. These ancient passive systems must have assembled their mass very quickly and then rapidly quenched over a short time-scale. Despite this significant evidence for galaxy bimodality, it is not yet clear which quenching mechanisms are primarily responsible for shutting down star formation and transforming the blue star-forming spiral galaxies into ‘red-and-dead’ galaxies. A major focus of current research in astrophysics is to determine the nature of the dominant quenching mechanisms, the typical quenching time-scales and how galaxy quenching depends on key parameters such as stellar mass, environment and redshift.

It has long been thought that both internal and external processes can be responsible for quenching star formation in galaxies. [Peng et al. \(2010\)](#) showed for galaxies in the SDSS ( $z < 0.1$ ) and zCOSMOS ( $0.3 < z < 0.6$ ) that the effects of mass and environment are largely separable, implying that there are two distinct quenching processes at work: one that depends on galaxy mass (‘mass quenching’, which is mostly independent of environment) and one that

\* E-mail: jaat2@cam.ac.uk

depends on environment (‘environmental quenching’, which is mostly independent of mass).

Mass quenching corresponds to internal processes that quench star formation, with the effectiveness of the quenching mechanisms mainly depending on total galaxy mass. In the low mass regime, outflows driven by stellar feedback (stellar radiation, stellar winds or supernova explosions) are thought to be effective at reducing star formation, although they may not be sufficient to completely quench star formation (e.g. Larson 1974; Dekel & Silk 1986). The shallower potential wells of these low-mass galaxies mean that the gas is less strongly bound and hence escapes more easily in the form of outflows. On the other hand, AGN feedback is thought to be more effective at quenching massive galaxies. As massive galaxies tend to host more massive black holes which can reach larger AGN luminosities, these galaxies drive more powerful outflows that can clean the galaxy of its gas content (ejective feedback) and/or heat the surrounding circumgalactic medium via energy injection through radio jets and winds, which in turns results into diminished cold gas accretion, hence quenching by starvation (e.g. Fabian 2012; Cicone et al. 2014; King & Pounds 2015; Fluetsch et al. 2018). In addition, it is thought that infalling gas from the intergalactic medium (IGM) is shock-heated as it accretes on to galaxies with halo masses above  $10^{12} M_{\odot}$ , resulting in the heating of the halo gas, hence suppressing cold accretion on to the galaxy, therefore halting the supply of the fuel for star formation in galaxies (‘halo quenching’, e.g. Birnboim & Dekel 2003; Kereš et al. 2005; Dekel & Birnboim 2006).

Environmental quenching corresponds to external processes that quench star formation, through interactions between a galaxy and its environment, i.e. other galaxies or the intracluster medium (ICM). These physical processes preferentially operate in dense environments and hence can be more important for galaxies residing in clusters and groups rather than galaxies in the field. One example of environmental quenching is ram pressure stripping, which can occur when a satellite galaxy falls into a cluster. Gas in the interstellar medium (ISM) can be rapidly removed as the galaxy moves through the hot ICM, causing rapid quenching (e.g. Gunn & Gott, J. Richard 1972; Abadi et al. 1999). Alternatively, strong tidal interactions between two close companion galaxies can also lead to the removal of gas (‘harassment’, e.g. Farouki & Shapiro 1981; Moore et al. 1996). Additionally, galaxies plunging into the hot ICM are likely prevented from accreting further gas from the IGM, shutting down the fuel supply for star formation and effectively resulting in galaxy ‘starvation’, a process referred to as ‘strangulation’ (e.g. Larson et al. 1980; Van Den Bosch et al. 2008).

Large galaxy surveys allow the dependence of galaxy quenching on critical parameters, such as mass and environment, to be studied. Since different quenching mechanisms operate over different mass regimes and environments, the mass- and environment-dependence of galaxy quenching can reveal the relative importance of different quenching mechanisms, which puts valuable constraints on the nature of the primary quenching mechanism in the Universe. For example, observations have revealed that red, quiescent, early-type galaxies are preferentially found in dense environments, while blue, star-forming late-type galaxies dominate the galaxy population in low-density environments (e.g. Dressler 1980; Balogh et al. 2004; Baldry et al. 2006; Peng

et al. 2012), suggesting that the environment could play a significant role in galaxy quenching. However, this prevalence of star-forming galaxies in low-density environments could also be a mass-dependent effect, as star-forming galaxies are preferentially low-mass, and there are more low-mass galaxies in low density environments, hence large samples of galaxies are needed to break the degeneracy between mass and environment (e.g. Peng et al. 2010).

Studies have also shown that star-forming galaxies occupy a tight relation (sometimes referred to as the ‘Main Sequence’) in the star formation rate–stellar mass plane up to  $z \sim 2$  (e.g. Daddi et al. 2007; Elbaz et al. 2007; Noeske et al. 2007; Renzini & Peng 2015). The small scatter in this relation suggests that merger-driven starbursts do not play a significant role in galaxy evolution but rather that slow, secular processes dominate the star formation process in galaxies.

Additional insights into galaxy quenching have come from detailed studies of the chemical content of galaxies. Since the abundance of metals in the ISM results from stellar nucleosynthesis, and is affected by the accretion of gas from the IGM as well as the ejection of material through galactic winds, the metallicity of a galaxy is a tracer for both the full star formation history and the flow of baryons into and out of the galaxy. Hence measurements of gas-phase and stellar metallicities can serve as a powerful method to constrain galaxy evolutionary processes and the relative importance of different quenching mechanisms. For example, observations have revealed that local galaxies follow a clear correlation between stellar mass and gas-phase metallicity, with the more massive galaxies being more metal enriched (e.g. Tremonti et al. 2004). Although it is not entirely clear what physical processes drive the mass-metallicity relation (MZR), it has been thought to primarily arise from supernova-driven galactic outflows of metal-rich gas which are preferentially expelled from low-mass galaxies (e.g. Larson 1974; Tremonti et al. 2004). Furthermore, observations of distant galaxies have revealed that the MZR holds at least out to  $z \sim 3$  (e.g. Erb et al. 2006; Maiolino et al. 2008; Mannucci et al. 2009), with the normalisation of the MZR decreasing with redshift, which could potentially be indicating that high-redshift galaxies were more strongly accreting pristine (low-metallicity) gas from the IGM, or perhaps that these galaxies are less evolved, and so have transformed less of their gas into stars, resulting in a lower amount of metals and hence a smaller metallicity. Furthermore, studies investigating the scatter in the MZR have revealed that the gas metallicity also has a secondary dependence on SFR. This three dimensional relationship between stellar mass, gas metallicity and SFR is known as the fundamental metallicity relation (FMR, Mannucci et al. 2010). For galaxies of a given stellar mass, the metallicity decreases with increasing SFR (e.g. Mannucci et al. 2010; Lara-López et al. 2010; Cresci et al. 2012). This anti-correlation is thought to be primarily driven by inflows of pristine gas, where the accreted gas dilutes the gas metallicity but also boosts the star formation rate by increasing the gas content. The small scatter in the FMR suggests that there is a smooth secular connection between star formation and gas flows.

Stellar metallicities offer a complementary method for studying the chemical enrichment of galaxies. Studies of local galaxies have revealed a stellar mass–stellar metallicity

relation (e.g. Gallazzi et al. 2005; Thomas et al. 2005; Panter et al. 2008; Thomas et al. 2010), where more massive galaxies typically have higher stellar metallicities. Comparisons of gas and stellar metallicities show that the stellar metallicities are typically 0.25 dex lower than the metallicity of the gas (e.g. Finlator & Dave 2008; Halliday et al. 2008; Peng & Maiolino 2014b; Pipino et al. 2014). Lian et al. (2018a,b) simultaneously analyse the gas and stellar MZR of local star-forming galaxies and find that, due to the relatively low stellar metallicity in low-mass galaxies, both MZRs can only be reproduced simultaneously if the metal-enrichment in low-mass galaxies is suppressed at early times in their evolution. This suppression can be achieved with either a time-dependent metal outflow with larger metal loading factors in galactic winds at early times (i.e. less metal retention), or through a time-dependent IMF, with steeper IMF slopes at early times (i.e. less metal production). More recent observations have begun to probe the stellar metallicities of high-redshift galaxies (e.g. Halliday et al. 2008; Sommariva et al. 2012; Gallazzi et al. 2014). However, these studies at high redshift currently lack the statistics to confirm the existence of a tight MZR. One significant benefit of studying stellar metallicities is that they can also be reliably measured for passive galaxies, thus making it possible to compare the metallicities of star-forming and passive galaxies. Such comparisons are currently not possible for gas metallicities, as the nebular emission in passive galaxies is often too weak (due to the lack of gas) to derive reliable gas-phase metallicities and also because proper calibration of metallicity diagnostics for the gas phase in non star-forming regions are not available.

Peng et al. (2015, P15 hereafter) pioneered the idea that the stellar metallicity difference between star-forming and passive galaxies can be used to determine the nature of the primary quenching mechanism in the Universe. During the evolution of a star-forming galaxy, gas is converted into stars and metals are continuously released into the ISM. As a result, subsequent generations of stars that form have progressively higher metallicities. However, due to the diluting effect of the accreting (pristine/low-metallicity) gas, the metallicity increase is modest. If at some point star formation is rapidly halted because of gas removal (ejective mode), then few metals and few stars are formed in the quenching phase and the resulting passive galaxy has the same stellar mass and stellar metallicity as its star-forming progenitor. If, instead, gas accretion on to the galaxy is halted by some mechanism (e.g. halo heating), hence resulting in quenching by starvation, then the galaxy keeps forming stars with the gas reservoir still available in the ISM, but the dilution effect from the accreting gas is no longer present and this results in a much steeper increase of the metallicity (and of the newly formed generations of stars) during the quenching phase; the result is a passive galaxy with slightly higher stellar mass and much higher stellar metallicity than the star-forming progenitor.

In their study, P15 analysed the stellar metallicities of 26,000 galaxies in SDSS DR4 (Adelman-McCarthy et al. 2006). At  $M_* < 10^{11} M_\odot$  passive galaxies were found to have a systematically larger stellar metallicity than star-forming galaxies of the same stellar mass, a clear signature of quenching by starvation. These observed differences in stellar metallicity between star-forming and passive galaxies

were then compared with the predictions of gas-regulator models in order to put quantitative constraints on the possible quenching mechanisms and time-scales. Their analysis confirmed that starvation (i.e. the halting of the supply of cold gas) is the primary mechanism responsible for shutting down star formation in galaxies with stellar masses below  $10^{11} M_\odot$ . P15 inferred a typical mass-independent quenching time-scale of 4 Gyr. They further found that their models are unable to reproduce the observed stellar metallicity differences when outflows are included, suggesting that outflows play a minor role in quenching galaxies. In order to distinguish between different origins for the starvation mechanism (e.g. halo quenching, strangulation or the shutdown of cosmological gas accretion), an analysis of the environmental dependence of the stellar metallicity difference was also undertaken. Satellite galaxies were found to have slightly higher metallicity differences than central galaxies at stellar masses below  $10^{10} M_\odot$ , suggesting an environmental origin for the starvation mechanism in this low-mass regime. However, at stellar masses above  $10^{10} M_\odot$  no difference was found between satellites and centrals (neither in terms of overdensity), suggesting that in this higher mass range environmental effects do not contribute significantly to the quenching.

The metallicity difference between passive and star-forming galaxies found by Peng et al. (2015) was also investigated by Spitoni et al. (2017) in the context of their exponentially declining accretion scenario. They interpret the difference in terms of a faster decline of the accretion, which is qualitatively very similar to the more abrupt halt of accretion adopted by Peng et al. (2015), hence independently confirming the need of a starvation phase to explain the metallicity difference between the two galaxy populations.

In this work we build upon the original analysis by P15, using stellar metallicity differences to determine the primary mechanism responsible for quenching star formation as a function of mass, environment and redshift. We make use of the larger spectroscopic sample of galaxies (930,000 cf. 566,000 in the original work) in SDSS DR7 (Abazajian et al. 2009) to further investigate galaxy quenching, utilising the increased statistical power to reduce statistical uncertainties and to extend the stellar metallicity analysis to green valley galaxies. Our analysis focusses on studying the mass-weighted stellar metallicities and stellar ages of galaxies, which can be directly compared with the predictions from gas regulator models. This approach is different from the original Peng et al. (2015) work, which studied light-weighted stellar metallicities and stellar ages. These light-weighted quantities trace the properties of the younger stellar populations within a galaxy and are more difficult to robustly compute within a gas regulator model, requiring detailed stellar population synthesis modelling that was not performed in the original work. We refine the gas regulator models used to compute the evolution in stellar metallicity during quenching, which allows a better assessment of the role of different quenching mechanisms to be made. We study the quenching of the progenitors of local passive galaxies, which began quenching around cosmic noon, utilising the observed stellar metallicity differences to determine the mechanisms responsible for shutting down star formation in these ancient systems. We also investigate the processes responsible for shutting down star formation in the

local Universe by analysing the properties of the green valley galaxy population. We investigate environmental quenching by studying the role of the central–satellite dichotomy as well as the local overdensity.

The paper is structured as follows. In Section 2, we describe our galaxy sample and the parameters used in our study. In Section 3, we outline how the differences in stellar metallicity between star-forming and passive (or green valley) galaxies can be used to distinguish between different quenching mechanisms. We also show the stellar mass–stellar metallicity relations which form the basis for all of our subsequent analysis. In Section 4 we describe the gas regulator models that are used to interpret the observed stellar metallicity differences. In Section 5 we compare the observed stellar metallicity differences with the predictions from gas regulator models to put constraints on the nature of the primary quenching mechanism and its associated quenching time-scale. In Section 6 we study the dependence of galaxy quenching on the environment, in terms of the central–satellite dichotomy as well as the local overdensity. In Section 7, we summarise our main findings and conclude.

## 2 DATA

### 2.1 Sample

We use the spectroscopic sample of galaxies in the Sloan Digital Sky Survey Data Release 7 (SDSS DR7, York et al. 2000; Abazajian et al. 2009) dataset, obtained using the Sloan 2.5m telescope (Gunn et al. 2006). Briefly, the SDSS DR7 dataset includes five-band photometry ( $u, g, r, i, z$ , Gunn et al. 1998; Doi et al. 2010) for 357 million distinct objects and spectroscopy (Smee et al. 2013) for over 1.6 million sources, including 930,000 galaxies which we study in our analysis. The spectroscopic sample of galaxies is substantially larger than the 566,000 galaxies in DR4 (Adelman-McCarthy et al. 2006) that were studied by P15. The galaxies chosen for spectroscopic follow-up consist of two main samples. Firstly, a sample complete to a Petrosian (1976) magnitude limit of  $r = 17.77$  (‘Main Galaxy Sample’, Strauss et al. 2002). Secondly, two smaller and deeper samples of luminous red ellipticals up to  $r = 19.2$ , corresponding to an approximately volume-limited sample to  $z = 0.38$  and  $z = 0.55$ , respectively (‘Luminous Red Galaxy Sample’, Eisenstein et al. 2001). Spectroscopic observations are in the optical/NIR (3800–9200 Å), have a spectral resolution  $R \sim 2000$  and a typical signal-to-noise ratio (S/N)  $\sim 10$  for galaxies near the main sample flux limit. Since the SDSS sample suffers from incompleteness at  $M_* < 10^{10} M_\odot$ , we apply the  $V_{\max}$  weightings from Blanton et al. (2003) to correct for volume incompleteness, allowing our analysis to be safely extended down to  $M_* = 10^9 M_\odot$ . However, we do note that these  $V_{\max}$  corrections only have a very minor effect on our stellar mass–stellar metallicity and stellar mass–stellar age relations, and so do not affect the results from our study.

We restrict our analysis to galaxies with reliable spectroscopic redshifts in the range  $0.02 < z < 0.085$ . This redshift cut was applied for several reasons. Firstly, we wish to reduce the effect of cosmological evolution on our analysis ( $z_{\max} \sim 0.55$  in the full SDSS sample corresponds to roughly 40 per cent of the age of the Universe). Secondly, we restrict

the redshift range to reduce the impact of aperture effects associated with the projected physical aperture of the SDSS spectroscopic fibre. If a broader redshift range were used, then the more distant galaxies would be studied over much larger effective radii than nearby galaxies, which could result in unwanted biases in our analysis. Finally, we restrict the redshift range to ensure that the  $V_{\max}$  correction remains reliable for the sample studied.

We also restrict our study to galaxies with reliable stellar metallicities and stellar ages, requiring that the median signal-to-noise ratio per spectral pixel is higher than 20. Such a high S/N cut could potentially introduce biases into our analysis as low surface brightness galaxies are preferentially removed from the sample. However, we find that the trends seen in our results do not change significantly with the chosen S/N criterion. Hence we have selected a S/N threshold of 20, since this provides a healthy balance between good statistics and reliability of measurements.

### 2.2 Derived Parameters

We use the spectral fitting code FIREFLY (Comparat et al. 2017; Goddard et al. 2017b; Wilkinson et al. 2017) to obtain stellar metallicities and stellar ages for each galaxy in the SDSS sample. Briefly, FIREFLY is a  $\chi^2$  minimisation fitting code that fits input galaxy spectra using an arbitrarily weighted, linear combination of simple stellar populations (SSPs) which can have a range of metallicities and ages. The weighted sum of metallicities and ages of each of the SSPs is used to derive the stellar metallicity and stellar age of the galaxy. The code returns both light-weighted and mass-weighted stellar ages and stellar metallicities. The light-weighted properties are obtained by weighting each SSP by its total luminosity across the fitted wavelength range (3500–7429 Å). On the other hand, mass-weighted properties are obtained by weighting each SSP by its stellar mass contribution. These two weightings are complementary. The light-weighted quantities primarily trace the properties of the younger stellar populations, as these tend to be brighter and dominate the light in the galaxy spectrum. On the other hand, the mass-weighted quantities trace the cumulative evolution of the galaxy. We study the mass-weighted ages and metallicities in our analysis, as these are directly comparable with our simple gas regulator models. This is in contrast with the light-weighted ages and metallicities, which in the model would have to be computed using detailed stellar population synthesis modelling, that assesses the evolution of the relative light contributions from different stellar populations across the fitted wavelength range.

FIREFLY fits the observed galaxy spectra using the stellar population models of Maraston & Strömbäck (2011), together with input stellar spectra from the empirical stellar library MILES (Sanchez-Blazquez et al. 2006) and a Kroupa IMF (Kroupa 2001). We have chosen to use MILES in our analysis as it had the most comprehensive sampling range in stellar metallicity and stellar age out of the empirical libraries that were available. The MILES library has metallicities  $[Z/H] = -2.3, -1.3, -0.3, 0.0, 0.3$  and ages that span from 6.5 Myr to 15 Gyr. The spectral resolution is 2.5 Å FWHM and the wavelength coverage is 3500–7429 Å. We have also repeated our analysis using the Salpeter (Salpeter 1955) and Chabrier (Chabrier 2003) IMFs and find that our



results are essentially unchanged. We have chosen to use the Kroupa IMF in this work.

We make use of the publicly available MPA-JHU DR7 release of spectral measurements<sup>1</sup>, which provides derived galaxy parameters for all galaxies in SDSS DR7. Stellar masses are obtained from fits to the photometry, using the Bayesian methodology of Kauffmann et al. (2003). Star formation rates within the spectroscopic fibre aperture are computed from the H  $\alpha$  emission (Brinchmann et al. 2004), which are then aperture-corrected using photometry (Salim et al. 2007) to obtain total SFRs which extends beyond the spectroscopic fibre aperture. We use the total SFRs in our analysis. For AGN or galaxies with faint emission lines, such as passive galaxies, SFRs are obtained from photometry. It should be noted that the SFRs derived for passive galaxies are most likely upper limits.

### 2.3 Environment

In order to study the dependence of galaxy quenching on environment, we divide the galaxy population into centrals and satellites, using the galaxy group catalogue of Yang et al. (2005, 2007). Briefly, the catalogue is constructed using an iterative Friend-of-Friends algorithm that has been calibrated on mock catalogues (Yang et al. 2005). Galaxies that are sufficiently close in projected distance and redshift are initially assigned into tentative groups. The properties of the dark matter halo (e.g. halo mass, size, velocity dispersion) associated with each tentative group are determined and this information is then used to update group memberships. The halo properties are recomputed, and this procedure is repeated until there are no further changes to the group membership. There are three different group samples that are constructed from these galaxies. Sample I contains 599,451 galaxies with SDSS redshifts only. Sample II contains 602,729 galaxies and includes the Sample I galaxies as well as additional galaxies whose redshifts were obtained from alternative surveys. Finally, Sample III contains 639,555 galaxies and includes the Sample II galaxies as well as additional galaxies that lack redshifts due to fiber collisions and are assigned redshifts of their nearest neighbours. For each sample, two group catalogs are constructed from the ‘Petrosian’ and ‘Model’ absolute magnitudes of the galaxies in the NYU-VAGC, respectively. We make use of Sample I with the ‘Model’ magnitudes. We find that using the other sample and magnitude combinations has no significant effect on our results.

Having established groups and group membership we then determine whether galaxies are centrals or satellites. Central galaxies are defined to be the most massive and the most luminous (in the  $r$ -band) in their group. All other members of the group are defined to be satellite galaxies. We do not take the galaxy’s spatial position in the group into account in our central–satellite classification system. Under the central–satellite definitions that we have used, isolated galaxies are always classified as centrals. Since there are a large number of isolated galaxies in the Yang et al. (2007)

group catalogue, a significant fraction of the central galaxies in our study are isolated centrals.

To further study the role the environment plays in quenching galaxies, we investigate the dependence of galaxy quenching on the local overdensity, which is a dimensionless density contrast given by  $\delta_i = (\rho_i - \rho_m)/\rho_m$ , where  $\delta_i$  is the overdensity around the  $i^{\text{th}}$  galaxy,  $\rho_i$  is an estimate of the local density around the  $i^{\text{th}}$  galaxy and  $\rho_m$  is the mean density at that redshift. We use the overdensities estimated by Peng et al. (2010), which were computed following the methodology developed by Kovač et al. (2010). For each galaxy, the projected distance to the fifth nearest neighbour  $d_5$  is determined. We then count the number of galaxies per unit volume contained within a cylinder of radius  $d_5$ , centred on the galaxy and with length  $\pm 1000 \text{ km s}^{-1}$ . The local overdensity is then given by the number of galaxies per unit volume contained within this cylinder.

## 3 METHOD AND RESULTS

### 3.1 Stellar metallicity

P15 pioneered the idea that stellar metallicities can be used to distinguish between different quenching mechanisms. We build upon this idea in our analysis. Although already briefly mentioned in the introduction, here we discuss the basic idea behind the approach in more detail. Consider a typical star-forming galaxy that is evolving along the main sequence, with its gas reservoir in near equilibrium, where gas depletion (e.g. through star formation and galactic winds) is balanced by gas replenishment through accretion. Over time, the stellar mass of the galaxy increases as new stars are formed out of the ISM. Furthermore, both the gas-phase metallicity and the stellar metallicity increase with time, as the elements produced through stellar nucleosynthesis enrich the ISM and increase the gas metallicity, which causes successively more metal-rich stars to form out of the gas, resulting in a steady increase in the stellar metallicity. While a galaxy evolves along the star-forming main sequence, it accretes an appreciable amount of gas from the IGM to fuel its star formation and maintain its gas reservoir in a rough equilibrium. Since this accreted gas is pristine (i.e. low metallicity), the metal content within the galaxy is diluted, and so the rate of metal enrichment is slowed down, with both the gas-phase metallicity and the stellar metallicity growing less steeply (per unit stellar mass formed) than would have been the case in the absence of any gas accretion. However, star-forming galaxies do not remain on the main sequence indefinitely. Indeed, the star-forming progenitors of passive galaxies must have been thrown off of the main sequence at some epoch, at which point their gas reservoir begins to decline, star formation shuts down, and a quiescent system is ultimately produced. We imagine that this quenching process begins at some time  $t_q$ , when the galaxy is thrown out of equilibrium and begins quenching. During this quenching phase both the stellar mass ( $\Delta M_*$ ) and the stellar metallicity ( $\Delta Z_*$ ) of the galaxy grow with time, as new metal-rich stars form out of the gas.

The amount by which the stellar metallicity is enhanced during quenching depends on the quenching mechanism.

Galaxies that quench rapidly through powerful outflows

<sup>1</sup> The MPA-JHU data release is available at <https://www.mpa.mpg.de/SDSS/DR7/>.

driven by AGN-feedback or ram pressure stripping quickly deplete their gas reservoirs and so only a small number of metal-enriched stars are produced during the quenching phase. In this case the stellar metallicity is only enhanced by a small amount during quenching and the stellar mass increase is negligible. Hence  $\Delta Z_*$  and  $\Delta M_*$  are small.

On the other hand, galaxies that deplete their gas reservoirs over long time-scales and quench slowly, e.g. through starvation (in the absence of outflows), produce a significant amount of metal-enriched stars during the quenching phase. More importantly, as was mentioned earlier, accretion of pristine gas from the IGM dilutes the metal content of the ISM and therefore reduces the rate at which the gas-phase and stellar metallicity can grow. In galaxies that quench through starvation, the supply of cold gas has halted. Since these galaxies therefore do not accrete any near-pristine gas from the IGM, both the gas-phase and the stellar metallicity grow more steeply with time. Combined with the fact that starvation also operates over a long quenching time-scale, this means that galaxies that quench through starvation undergo a significant increase in stellar metallicity during quenching, resulting in a large  $\Delta Z_*$ .

Since small stellar metallicity enhancements correspond to quenching by rapid gas removal and large enhancements correspond to starvation, it is possible to distinguish between the two quenching mechanisms by measuring the amount by which the stellar metallicity is increased ( $\Delta Z_*$ ) during the quenching phase. Of course, we cannot make this measurement directly as it is not possible to track the evolution of the stellar metallicity of an individual galaxy across cosmic time. Instead, we can measure this enhancement indirectly by statistically studying the difference in stellar metallicity between star-forming and passive galaxies. Star-forming galaxies represent galaxies prior to quenching ( $t < t_q$ ), while passive galaxies represent galaxies after quenching has completed. Hence the stellar metallicity enhancement during quenching can be inferred from the stellar metallicity difference between star-forming and passive galaxies. By measuring this stellar metallicity difference for many galaxies the nature of the primary mechanism responsible for shutting down star formation in galaxies can be determined.

### 3.2 Classification

We use the bimodality in the star formation rate–stellar mass (SFR– $M_*$ ) plane to classify galaxies as either star-forming, green valley or passive. In a similar fashion to [Renzini & Peng \(2015\)](#), we define the boundary of the star-forming (quenched) region in the SFR– $M_*$  plane by the locus of points, given by a best straight-line fit, where the number of star-forming (quenched) galaxies per SFR– $M_*$  bin has dropped below some threshold with respect to the peak value at a given mass. In this way, the SFR– $M_*$  plane is partitioned into three regions, which correspond to star-forming, green valley and passive galaxies, respectively. The adopted boundary between star-forming and green valley galaxies is given by

$$\log \text{SFR} = 0.70 \log M_* - 7.52 \quad (1)$$

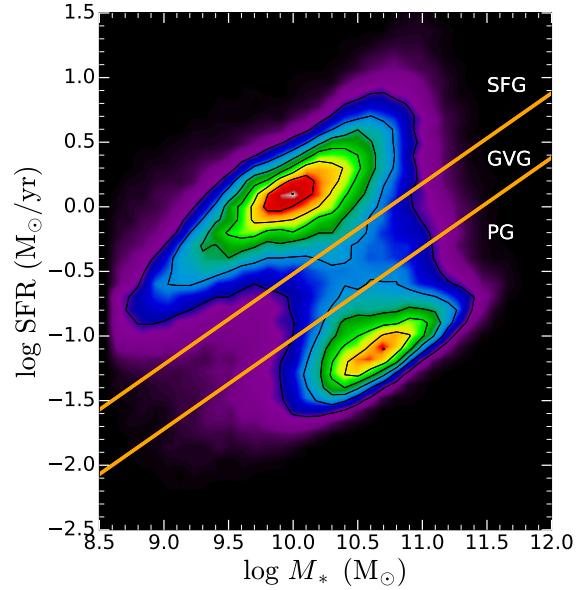


**Figure 1.** The bimodality of local galaxies in the star formation rate–stellar mass (SFR– $M_*$ ) plane. We only show the subsample of SDSS DR7 galaxies in the redshift range  $0.02 < z < 0.085$ . The colour shown reflects the number of galaxies in each SFR– $M_*$  bin, ranging from low counts (purple) to high counts (red). The orange lines mark the boundaries of the star-forming, green valley and passive regions of the plane. Galaxies in the upper left are classified as star-forming (SFG), intermediate galaxies are classified as green valley (GVG), and galaxies in the lower right are classified as passive (PG).

and the adopted boundary between green valley and passive galaxies is given by

$$\log \text{SFR} = 0.70 \log M_* - 8.02. \quad (2)$$

This selection criterion is illustrated in Fig. 1, where we show the subsample of SDSS DR7 galaxies in the redshift range  $0.02 < z < 0.085$ . It should be noted that the results from our analysis do not change significantly when the slopes or intercepts of the boundaries between the star-forming, green valley and passive regions are changed.

Star-forming galaxies are also required to have their BPT classification set to ‘star-forming’ according to the [NII]–BPT diagnostic diagram ([Brinchmann et al. 2004](#)). This excludes objects hosting an AGN, ensuring that we only analyse true star-forming galaxies in our study (as the presence of the AGN may affect the estimation of the star formation rate, through its additional contribution to the nebular line emission, and may also affect the determination of the stellar metallicity through the additional contribution to the continuum emission). After applying our cuts on redshift, S/N and this selection criterion, our final sample consists of 16,685 star-forming galaxies, 8,445 green valley galaxies and 53,661 passive galaxies. All of these galaxies have reliable stellar masses, star formation rates, stellar metallicities and stellar ages.

Note that the relative fraction of star-forming, green valley and passive galaxies does not reflect the real relative census of these different populations of galaxies as their relative number is also convolved with our selection criteria (in

particular the requirement of high S/N on the continuum, to reliably measure the stellar metallicities).

### 3.3 Scaling relations

We now apply the previously discussed cuts in redshift and S/N, as well as the SFR- $M_*$  classification criterion to investigate relations between stellar mass and stellar metallicity, as well as stellar mass and stellar age, for star-forming, green valley and passive galaxies. All galaxies of a particular class (e.g. star-forming) are binned in stellar mass bins of 0.02 dex and the median stellar metallicity and stellar age in each mass bin is determined. Error bars on the median stellar metallicities and stellar ages are given by the  $1\sigma$  uncertainty on the median ( $1.253\sigma/\sqrt{N}$ ). We also apply a running average of 0.2 dex to smooth the data. These scaling relations in stellar mass–stellar metallicity and stellar mass–stellar age will form the basis for all of our subsequent analysis. The differences in stellar age between star-forming and passive (green valley) galaxies, will be used to estimate the epoch when the progenitors of local passive (green valley) galaxies began quenching. Furthermore, the differences in stellar metallicity between star-forming and passive (green valley) galaxies will enable us to determine which mechanism was primarily responsible for quenching the progenitors of local passive (green valley) galaxies.

#### 3.3.1 Stellar metallicity

The mass-weighted stellar mass–stellar metallicity relation for star-forming (blue), green valley (green) and passive galaxies (red) are shown in the top panel of Fig. 2. We find that the stellar metallicity increases with stellar mass for star-forming, green valley, and passive galaxies alike. This result is qualitatively similar to what has been seen in previous studies, where the stellar metallicity tends to increase with stellar mass. For example, Gallazzi et al. (2005) studied the light-weighted stellar mass–stellar metallicity relation for the total galaxy population (i.e. without distinguishing between star-forming, green valley and passive galaxies) in SDSS DR4 and found that more massive galaxies typically have larger stellar metallicities. P15 further divided the Gallazzi et al. (2005) sample into star-forming and passive galaxies, and found that the stellar metallicity tends to increase with stellar mass for both of these subpopulations. Similar to P15, but using mass-weighted rather than light-weighted stellar metallicities in our study, we also find that at a given stellar mass the stellar metallicity of passive galaxies is systematically larger than that of star-forming galaxies. Furthermore, the difference in stellar metallicity decreases with increasing stellar mass. In contrast with the initial P15 study however, we find that this large difference in stellar metallicity is present and highly significant also in massive galaxies with masses around  $10^{11} M_\odot$ . As we shall see later on, this metallicity difference is even higher if one compares the metallicity of passive massive galaxies with the metallicity of their progenitors at high redshift. This significant difference in stellar metallicity between star-forming and passive galaxies is qualitatively consistent with quenching through starvation, and inconsistent with quenching through simple gas removal (ejective mode). Within the

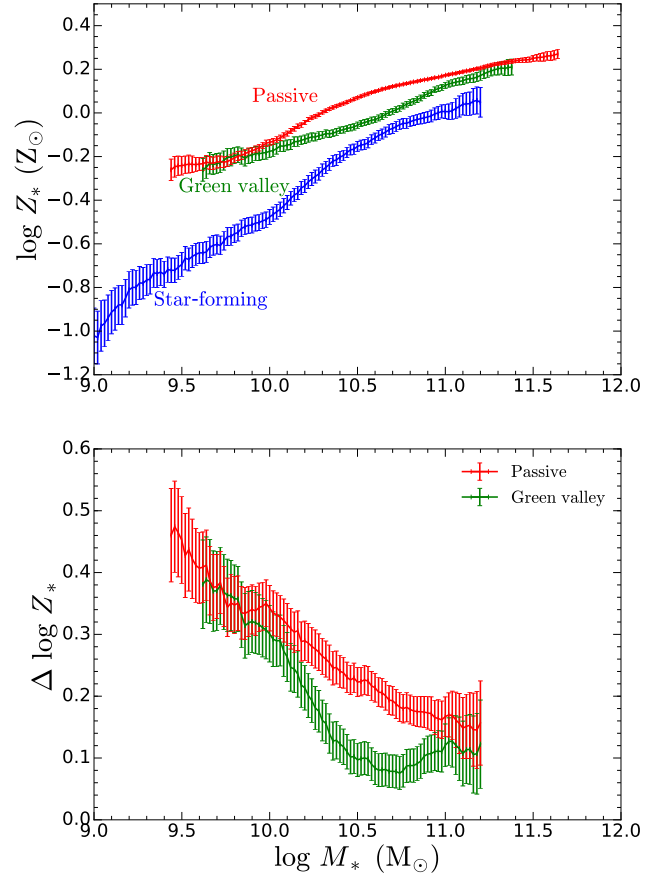


**Figure 2.** Top panel: The stellar mass–stellar metallicity relation for star-forming (blue), green valley (green) and passive (red) galaxies. Galaxies are binned in 0.02 dex stellar mass bins and the median stellar metallicity in each bin is plotted. Error bars correspond to the  $1\sigma$  uncertainty on the median. Bottom panel: The observed difference in stellar metallicity between star-forming and passive galaxies (red), as well as the difference between star-forming and green valley galaxies (green). Error bars represent the  $1\sigma$  error on the stellar metallicity difference.

starvation scenario, the decrease in stellar metallicity difference with mass can be attributed to the smaller gas fractions present in more massive galaxies, which therefore have relatively smaller amounts of gas available to convert into metals during starvation. Furthermore, we note that at the low-mass end the stellar metallicity of green valley galaxies and passive galaxies are similar, suggesting that low-mass green valley galaxies have already undergone the bulk of their chemical enrichment during the quenching phase. At high masses green valley galaxies have metallicities intermediate between star forming and passive; we will discuss the implications of these trends in terms of quenching scenarios and time-scales.

The difference in stellar metallicity between star-forming and passive galaxies (red), as well as the difference between star-forming and green valley galaxies (green) is shown in the bottom panel of Fig. 2. The stellar metallicity differences are computed by determining the logarithmic difference between the appropriate populations for each stellar mass bin. For example, the stellar metallicity difference between star-forming and passive galaxies is given by

$\log Z_{\text{QG}}(M_*) - \log Z_{\text{SFG}}(M_*)$ . As already mentioned, we find, similar to P15, that the stellar metallicity difference between star-forming and passive galaxies decreases with increasing stellar mass. However, in contrast to their study, we find that there is a non-zero difference in stellar metallicity above  $10^{11} M_{\odot}$ . This disagreement with the original study is most likely because we are using a different set of stellar metallicities. Our work relies upon the mass-weighted stellar metallicities obtained using FIREFLY, which traces the cumulative evolution of a galaxy, while their analysis used the light-weighted stellar metallicities from Gallazzi et al. (2005), which traces the properties of the younger stellar populations and is more sensitive to recent star formation. Due to the lack of recent star formation in passive galaxies, there are no young stellar populations present that would dominate the spectrum, and so the light-weighted and mass-weighted stellar metallicities of passive galaxies are comparable. On the other hand, since young stellar populations are present in star-forming galaxies, the light-weighted stellar metallicities are typically larger than the mass-weighted stellar metallicities, as the light-weighted properties are more strongly weighted towards the younger, more metal-rich stellar populations. Hence the mass-weighted stellar metallicity difference between star-forming and passive galaxies should be larger than the light-weighted stellar metallicity difference, explaining why we find a non-zero stellar metallicity difference even at high masses in our study. This non-zero stellar metallicity difference around  $10^{11} M_{\odot}$  (which we will show to be even larger when comparing passive galaxies with their high-redshift star-forming progenitors), will make it possible to determine the nature of the primary quenching mechanism for massive galaxies in our study, which is something that was not possible in the original P15 analysis.

### 3.3.2 Stellar age

We show the mass-weighted stellar mass–stellar age relation for star-forming, green valley and passive galaxies in Fig. 3. The stellar ages of the different galaxy subpopulations tend to increase with increasing stellar mass. Furthermore, passive galaxies and green valley galaxies are always systematically older than star-forming galaxies of the same stellar mass. We note that the mass-weighted ages for star-forming and passive galaxies in our study are roughly 2 Gyr higher than the light-weighted ages in P15. This could be due to the fact that we study mass-weighted rather than light-weighted ages (mass-weighted ages should be larger), or because the stellar ages we use were obtained using a different spectral fitting code. Fig. 3 also shows the stellar age difference  $\Delta t$  between star-forming and passive galaxies, as well as the age difference between star-forming and green valley galaxies. We find that the star-forming–passive age difference is roughly mass-independent at  $\sim 4.5$  Gyr (consistent with the  $\sim 4$  Gyr in P15), while the star-forming–green valley age difference is roughly mass-independent at  $\sim 2.5$  Gyr.

## 4 MODEL

In order to put constraints on the nature of the primary quenching mechanism, we compare the observed stellar metallicity differences between star-forming and passive (or

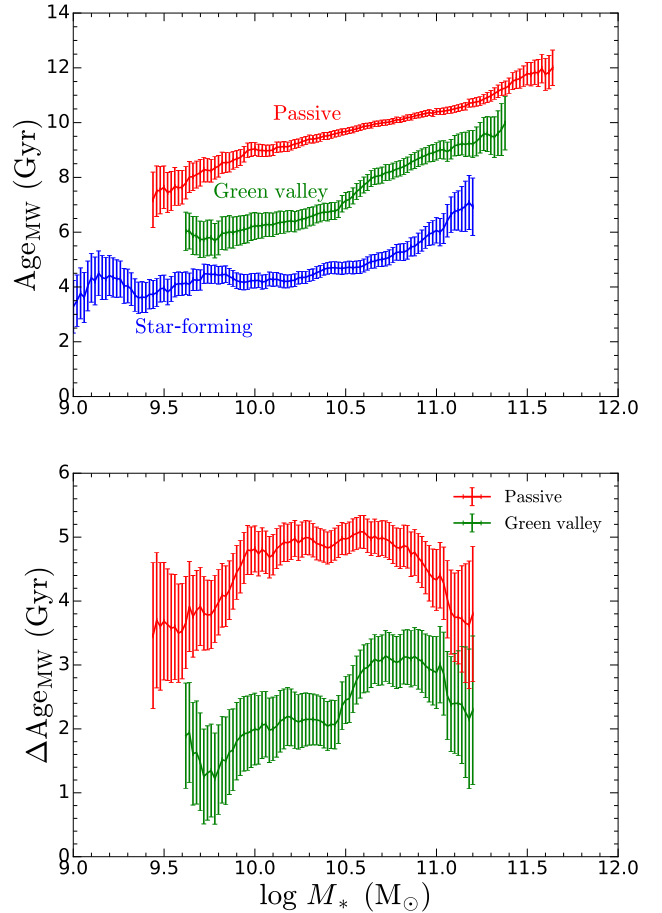


**Figure 3.** Top panel: The stellar mass–stellar age relation for star-forming (blue), green valley (green) and passive (red) galaxies. Bottom panel: The observed difference in stellar age between star-forming and passive galaxies (red), as well as the difference between star-forming and green valley galaxies (green).

green valley) galaxies with the predictions made by analytical models for galaxy evolution. In this section we discuss the models we use to determine how the stellar metallicity of a galaxy changes during quenching. There are three key factors that influence our model predictions. Firstly, our results depend on the differential equations that we solve to determine the evolution of the mass and metallicity of gas and stars in the galaxy. Secondly, we must estimate the cosmic epoch when the progenitors of local passive (or green valley) galaxies began quenching. Finally, we must specify the initial properties these star-forming progenitors had at the onset of quenching.

### 4.1 Differential Equations

We make use of the analytical framework developed in the gas regulator model of Peng & Maiolino (2014b), which does not assume any equilibrium conditions for galaxy evolution. Star formation is regulated, near equilibrium by the mass of the gas reservoir, which itself is affected by ongoing star formation, gas accretion and gas outflows. Furthermore, the ISM is enriched by metals produced through stellar nucleosynthesis, it is diluted by accretion of gas from the IGM



(assumed to be near pristine) and metals are removed from the galaxy in galactic winds.

We use the instantaneous recycling approximation (IRA), which assumes that massive stars instantly die upon formation, returning some fraction of their (chemically enriched) gas to the ISM. Furthermore, this enriched material is instantaneously mixed uniformly with the gas in the ISM. On the other hand, low-mass stars are assumed to remain on the main sequence indefinitely, returning zero material to the ISM. Our model only tracks the global evolution of the stars and gas in the galaxy, and does not consider the spatial dependence of gas flows, metal enrichment or star formation. We also assume that the IMF does not change with time.

We parametrize star formation through an integrated, linear ( $n = 1$ ) Schmidt-Kennicutt law (Schmidt 1959; Kennicutt 1998), with the star formation rate  $\Psi$  directly proportional to the gas mass  $g$ . That is,

$$\Psi = \epsilon g, \quad (3)$$

where  $\epsilon$  is the ‘star formation efficiency’. Although there is still debate on whether the Schmidt-Kennicutt relation is linear or super-linear, we assume the linear approximation in our model. We use the total gas mass for  $g$ , which includes both the atomic and molecular components. Furthermore, we use the total star formation efficiency for  $\epsilon$ , which again takes both the atomic and molecular components into account. We assume that  $\epsilon$  remains constant during quenching. The star formation efficiency is related to the total gas depletion time-scale  $t_{\text{depl}}$ , through  $\epsilon = 1/t_{\text{depl}}$ . The depletion time-scale is defined as the time needed to convert the entire reservoir of gas in the galaxy into stars, assuming that the star formation rate remains fixed at the current value. We explore how our model predictions change when only the molecular gas component is considered in Appendix A.

We assume that the mass outflow rate  $\Lambda$  is directly proportional to the star-formation rate,

$$\Lambda = \lambda_{\text{eff}} \Psi, \quad (4)$$

where  $\lambda_{\text{eff}}$  is the so-called outflow ‘effective’ mass-loading factor. The term ‘effective’ refers to the outflowing mass that effectively escapes the galaxy (i.e. permanently removed from the system) or which is reaccreted by the galaxy only on very long time-scales ( $\geq$  Hubble time). Outflowing gas which is reaccreted on to the galaxy on short time-scales is not accounted into the outflowing budget, as it is effectively recycled for further star formation. Therefore, galaxies with prominent outflows, and with (‘classical’) outflow loading factor  $\lambda > 0$ , may still have  $\lambda_{\text{eff}} = 0$  if the outflow does not escape the galaxy or the halo (as seems to be the case for many massive galaxies, Fluetsch et al. 2018).

In our subsequent analysis we will be modelling quenching purely through starvation (no inflow and no ‘effective’ outflows, i.e. with  $\lambda_{\text{eff}} = 0$ ), as well as quenching through a combination of starvation and outflows (i.e. no inflow and  $\lambda_{\text{eff}} > 0$ ).

Gas flows and star formation can change the amount of gas contained within a galaxy. Star formation and galactic winds deplete the gas reservoir, while gas accretion replenishes it. For a galaxy forming stars at a rate  $\Psi$ , ejecting gas at a rate  $\Lambda$  and accreting material at a rate  $\Phi$ , the evolution

of the gas mass is given by

$$\frac{dg}{dt} = -(1 - R)\Psi - \Lambda + \Phi. \quad (5)$$

Here  $R$  is the return fraction, which is the fraction of the mass of newly formed stars that is quickly returned (IRA) to the ISM through stellar winds and supernovae.  $1 - R$  represents the fraction of mass that is locked up in long-lived stars and stellar remnants. We assume  $R = 0.425$  (Vincenzo et al. 2016a) in our analysis.

Gas flows and star formation also affect the metal content of a galaxy. The metals produced by stellar nucleosynthesis enrich the ISM, while the accretion of pristine gas dilutes it and galactic winds remove metals from the galaxy. In general, the evolution of the gas metallicity  $Z_g$  (Tinsley 1980) is given by

$$g \frac{dZ_g}{dt} = (1 - R)y\Psi - (Z_\Lambda - Z_g)\Lambda - (Z_g - Z_\Phi)\Phi, \quad (6)$$

where  $y$  is the net yield, representing the amount of newly-forged metals released into the ISM per unit mass locked up in long-lived stars.  $Z_\Lambda$  and  $Z_\Phi$  are the metallicity of the outflowing and inflowing gas, respectively.

Vincenzo et al. (2016a) showed that the value of the net yield is quite sensitive to the IMF, the IMF upper mass cutoff, as well as the set of stellar yields (which specify the dependence of the mass of metals released on the initial mass of a star) that are adopted. We assume the  $y = 0.054$  value corresponding to the Kroupa (2001) IMF, as this is the same IMF that was used to determine the observed stellar metallicities in FIREFLY. We do note that using a smaller yield value will affect our model predictions, as chemical enrichment is slower and so it will take longer to reproduce the observed stellar metallicity differences, resulting in a longer quenching time-scale. Furthermore, models using small  $y$  values that incorporate outflows will have more difficulty reproducing the observed stellar metallicity differences.

We will make the simplifying assumption that the metallicity of the outflowing gas and the metallicity of the ISM are equal ( $Z_\Lambda = Z_g$ ), i.e. we assume that outflows do not preferentially remove metals from the galaxy. However, this assumption may not be completely true for low-mass galaxies, as Lian et al. (2018a,b) find that some metal-loading in the outflow (relative to the ISM metallicity) is required to simultaneously match gas-phase and stellar metallicities. Vincenzo et al. (2016b) also find that preferential ejection of oxygen (and other core-collapse SNe products) provides a better description of the observed chemical abundances and metallicities. This is also observed in a few galactic outflows (e.g. Ranalli et al. 2008). However, this differential effect is not major and our simplified analysis, which does not include this effect, is expected to provide a good description of the overall metallicity evolution, especially, obviously, for the starvation scenario (in the outflow scenario the preferential ejection of metals makes an even stronger case for explaining the observed metallicity difference between passive and star-forming galaxies in terms of starvation).

Furthermore, we will be investigating the effect that starvation (the halting of gas accretion) has on the evolution of stellar metallicities. Hence we will assume that there is no gas accretion during the quenching period and we set the inflow rate  $\Phi = 0$ .

Under these set of assumptions, equations (5) and (6)

are simplified. The evolution of the gas mass is now given by

$$\frac{dg}{dt} = -(1-R)\Psi - \Lambda. \quad (7)$$

Furthermore, the evolution of the gas metallicity is now given by

$$\frac{dZ_g}{dt} = (1-R)y\epsilon, \quad (8)$$

which continues to grow with time as stars return their metal-enriched gas to the ISM.

The stellar mass of the galaxy continuously increases due to the conversion of gas into stars. The evolution of the stellar mass  $s$  is given by

$$\frac{ds}{dt} = (1-R)\Psi, \quad (9)$$

where  $(1-R)\Psi$  is the net star formation rate that contributes to the stellar mass increase of the galaxy.

Finally, the mass-weighted stellar metallicity rises with time as increasingly more metal-rich stars form out of the enriched gas. The evolution of the mass-weighted stellar metallicity is given by

$$\frac{dZ_*}{dt} = \frac{\Psi}{s} (1-R)(Z_g - Z_*). \quad (10)$$

The stellar metallicity is a weighted average of the metallicities of all the stars in the galaxy. Since galaxies consist of a mixture of old metal-poor stars that formed early on out of pristine gas, as well as young metal-rich stars that recently formed out of more enriched gas, the mass-weighted stellar metallicity traces the cumulative chemical evolution of the galaxy. On the other hand, the gas metallicity only traces the current state of chemical enrichment. As a result, the mass-weighted stellar metallicity of a galaxy tends to lag behind the gas metallicity.

## 4.2 Estimating the onset of quenching

Prior to the onset of quenching, the star-forming progenitors of local passive galaxies probably evolved along the star-forming main sequence, where their gas reservoir was kept relatively fixed due to the balance between the depletion of gas driven by star formation and galactic winds and the replenishment of gas by accretion. However, these progenitors must have started quenching at some cosmic epoch in order to form the passive galaxies we see in the local Universe. In our model we assume that these progenitors began quenching through starvation at a redshift  $z_q$ , which is the epoch when the accretion of gas is halted in the starvation scenario.

We assume that  $z_q$  depends on the stellar mass  $M_*$  of the local passive galaxies. Indeed, studies such as [Thomas et al. \(2005, 2010\)](#) have shown how the typical star formation epoch and time-scale depend on galaxy mass, finding that the more massive galaxies tended to form the bulk of their stars earlier on in cosmic history than less massive galaxies. Hence we would expect the progenitors of the most massive passive galaxies to have started quenching at higher redshift than the progenitors of low-mass passive galaxies. We use the mass-weighted stellar ages of local passive galaxies  $t_0(M_*)$  that were obtained in this work (see Fig. 3) to estimate the

epoch associated with the onset of quenching  $z_q$ . We make the simplifying assumption that a negligible amount of additional stellar mass is formed during the quenching phase, i.e. that the gas mass available for additional star formation is small compared with the mass of stars already assembled. Since galaxies that quench through starvation form additional stars during the starvation phase, the lookback times to the onset of quenching that we estimate here through the mass-weighted ages are actually underestimates. We will revisit this caveat in Section 5.2.1. Under this simplifying assumption there is a simple relationship between the stellar age of the local passive galaxy  $t_0(M_*)$  and the stellar age of its star-forming progenitor at the onset of quenching  $t(z_q, M_*)$ . The difference between these two ages is just given by the (mass-dependent) lookback time  $t_{lb}(M_*)$  to the onset of quenching. We have that

$$t_0(M_*) = t(z_q, M_*) + t_{lb}(M_*). \quad (11)$$

As discussed earlier, the star-forming progenitors of the most massive passive galaxies will have begun quenching at an earlier epoch in cosmic history, so these galaxies will have the largest lookback times. We therefore need to determine the epoch when these progenitors began quenching,  $z_q(M_*)$ , which is equivalent to determining the lookback time to the onset of quenching,  $t_{lb}(M_*)$ .

For local passive galaxies, it is reasonable to assume that the ages of their star-forming progenitors were much smaller than the lookback time to the onset of quenching, i.e.  $t(z_q, M_*) \ll t_{lb}(M_*)$ , as the stellar ages of the progenitors are usually  $< 1$  Gyr (see e.g. [Reddy et al. \(2012\)](#); [Sklias et al. \(2017\)](#) for massive galaxies at  $z = 1-3$ , and [Gallazzi et al. \(2014\)](#) for low-mass galaxies at  $z \sim 0.7$  if the observed relation is extrapolated down to lower masses), while the lookback times are usually  $\sim 10$  Gyr. In this case, the lookback times (and therefore  $z_q$ ) are simply given by  $t_0(M_*)$ , the stellar ages of the local passive galaxies. That is, we set  $t_{lb}(M_*) = t_0(M_*)$ .

For local green valley galaxies, we have to be more careful, as these are still in the quenching phase. In this case the ages of the progenitors are comparable to the lookback times, i.e.  $t(z_q, M_*) \sim t_{lb}(M_*)$ . In this case we estimate the lookback time,  $t_{lb}(M_*)$ , by assuming that the ages of the star-forming progenitors of the same mass,  $t(z_q, M_*)$ , are given by the stellar ages of local star-forming galaxies,  $t_{0,SFG}(M_*)$ . The lookback time to the onset of quenching is then given by the stellar age difference between local green valley galaxies and local star-forming galaxies of mass  $M_*$ , i.e.  $t_{lb}(M_*) = t_{0,GVG}(M_*) - t_{0,SFG}(M_*)$ .

We show the redshifts  $z_q$  when the star-forming progenitors of local passive and local green valley galaxies began quenching through starvation in our models in Fig. 4.

## 4.3 Initial conditions

In order to model the change in stellar metallicity during quenching, the initial state of the star-forming progenitor at the onset of quenching has to be specified. The key initial conditions in our model are the gas mass  $g$ , the gas metallicity  $Z_g$ , the stellar metallicity  $Z_*$  and the star formation efficiency  $\epsilon$ , i.e. the star formation rate per unit gas mass ( $\epsilon = \text{SFR}/M_{\text{gas}}$ ), often identified with the inverse of the depletion time-scale  $t_{\text{depl}}$ , i.e. the time required by the star

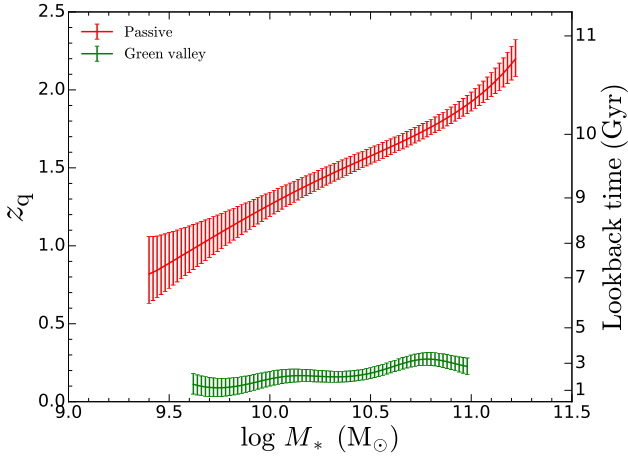


**Figure 4.** The redshift  $z_q$  when the star-forming progenitors of local passive galaxies (red) and local green valley galaxies (green) begin quenching through starvation, as a function of stellar mass, as inferred by our analysis. The onset of quenching for passive and green valley galaxies were estimated from the mass-weighted stellar ages of local passive galaxies, and the difference in mass-weighted stellar age between local green valley and local star-forming galaxies, respectively.

formation to deplete all available gas into stars, in the ideal case in which star formation remains constant and gas is not replenished. We use mass- and redshift-dependent scaling relations for star-forming galaxies, that span the stellar mass range  $\log(M_*/M_\odot) = 9.4\text{--}11.3$  and redshift range  $0 \leq z \leq 2.0$ , to determine the values for these quantities. We try, whenever possible, to use empirical scaling relations as opposed to theoretical scaling relations in our models.

In order to determine the total gas mass and star formation efficiency, we require measurements of both the molecular and atomic gas components. The total gas mass and total gas depletion times are simply given by the sum of the molecular and atomic masses, and the sum of the molecular and atomic depletion times, respectively. Tacconi et al. (2018) used a combination of CO and dust measurements to determine the molecular gas properties of star-forming galaxies over a broad range in stellar mass  $\log(M_*/M_\odot) = 9.0\text{--}11.9$  and redshift  $z = 0\text{--}4.4$ . We use their relations for molecular gas fractions (giving molecular gas masses) and molecular gas depletion time-scales (giving molecular star formation efficiencies) in our model. Due to the intrinsic faintness of HI in emission, there are currently no atomic gas measurements for star-forming galaxies within our required redshift range  $0.5 \leq z \leq 2.0$  (see e.g. Rhee et al. 2016; Cortese et al. 2017). We have chosen to use theoretical relations between the molecular and atomic components of galaxies to estimate atomic gas masses and atomic gas depletion times in our model, which are supported by indirect measurements. We use the results from Popping et al. (2014), who used pressure-based  $H_2$  formation recipes to determine the evolution of the molecular-to-atomic gas mass ratio  $R_{\text{mol}}$  across cosmic time, indicating that at high redshift, at least out to  $z \sim 3$ , most of the gas in a galaxy is in the molecular phase. These results are in agreement with HI constraints given by the (lack of) evolution of damped Ly  $\alpha$  absorption systems (Prochaska & Wolfe 2009), indicating that the amount of

HI in galaxies remains roughly constant out to  $z \sim 3$ , while the amount of molecular gas increases substantially (Tacconi et al. 2018). We estimate the atomic gas mass  $a$  in our model galaxies from the molecular gas mass  $m$  and  $R_{\text{mol}}$  by computing  $a = m/R_{\text{mol}}$ . In a similar fashion, the atomic depletion time  $t_{\text{depl},a}$  is obtained from the molecular depletion time  $t_{\text{depl},m}$  through  $t_{\text{depl},a} = t_{\text{depl},m}/R_{\text{mol}}$ .

In contrast with local passive galaxies, which are thought to have mostly begun quenching at higher redshift, local green valley galaxies are a transitional population that have only recently begun quenching. Therefore, in our analysis that investigates the quenching of star formation in local green valley galaxies, we use the local relations (Boselli et al. 2014) for the total gas mass and total gas depletion time measured for star-forming galaxies in our models. Since our models estimate that the star-forming progenitors of these green valley galaxies began quenching between  $0.15 \leq z_q \leq 0.25$  (based off of the stellar age difference between local star-forming and green valley galaxies), we evolve the  $z = 0$  relations to this redshift range, using the redshift-dependence of the gas mass and gas depletion time-scale measured by Tacconi et al. (2018).

Deep observations of galaxies have begun to probe the stellar mass–stellar metallicity relation at high redshift, such as the works by Choi et al. (2014) at  $z \sim 0.4$ , Gallazzi et al. (2014) at  $z = 0.7$ , Lonoce et al. (2015) and Onodera et al. (2015) at  $z \sim 1.5$ , Halliday et al. (2008) at  $z = 2$ , Sommariva et al. (2012) at  $z = 3$  and Lian et al. (2018c). However, current studies of the stellar metallicity relation at high redshift do not yet have the broad coverage in stellar mass and redshift, nor the statistics (resulting in very large scatter) that is required by our models. Therefore, we do not use the observed stellar mass–stellar metallicity relations at high redshift to determine the initial stellar metallicities in our model. Instead, we make the assumption that the gas MZR and stellar MZR of star-forming galaxies evolve similarly across cosmic time (Peng & Maiolino 2014b). In that case the evolution of stellar metallicity with redshift is simply given by the evolution of the gas metallicity. We have used the redshift evolution of the gas MZR measured by Maiolino et al. (2008) to evolve the local relation for mass-weighted stellar metallicities to higher redshift, and this is shown in Fig. 5.

Studies of gas metallicities can suffer from calibration issues, where different diagnostics can yield significantly different metallicities, resulting in mass–metallicity relations with different shapes and different normalisations (see discussion by e.g. Curti et al. 2017). We wish to avoid any issues associated with metallicity calibrations in our analysis. We could in principle use the stellar metallicities from FIREFLY and the gas metallicities from Maiolino et al. (2008), who estimated the evolution of the MZR as a function of redshift by using consistent calibrations within the gas-phase metallicity diagnostics. However, we would then be using two separate metallicity calibrations for gas and stars, which are likely to be inconsistent with one another. We restrict our analysis to a single calibration scheme and do not directly use the gas metallicities from Maiolino et al. (2008) in our model. Instead, we use only the metallicity evolution (i.e.  $\Delta \log Z_g / \Delta z$ ) inferred by Maiolino et al. (2008) and renormalize it locally using the stellar metallicities obtained by FIREFLY.

**Table 1.** Summary of the initial conditions and other key quantities used in the gas regulator model.

Quantity	Description	Passive galaxies	Green valley galaxies
$g$	Initial total gas mass (molecular and atomic)	Molecular gas mass: <a href="#">Tacconi et al. (2018)</a>	Molecular gas mass: <a href="#">Boselli et al. (2014)</a>
		Atomic gas mass: <a href="#">Popping et al. (2014)</a>	Atomic gas mass: <a href="#">Boselli et al. (2014)</a>
		Redshift-evolution: <a href="#">Tacconi et al. (2018)</a>	Redshift-evolution: <a href="#">Tacconi et al. (2018)</a>
$t_{\text{depl}} (= \epsilon^{-1})$	Total gas depletion time (molecular and atomic)	Molecular gas depletion time: <a href="#">Tacconi et al. (2018)</a>	Molecular gas depletion time: <a href="#">Boselli et al. (2014)</a>
		Atomic gas depletion time: <a href="#">Popping et al. (2014)</a>	Atomic gas depletion time: <a href="#">Boselli et al. (2014)</a>
		Redshift-evolution: <a href="#">Tacconi et al. (2018)</a>	Redshift-evolution: <a href="#">Tacconi et al. (2018)</a>
$Z_*$	Initial mass-weighted stellar metallicity	Local $Z_*$ : $Z_{\text{MW}}$ for star-forming galaxies from this work	Local $Z_*$ : $Z_{\text{MW}}$ for star-forming galaxies from this work
		Redshift-evolution: <a href="#">Maiolino et al. (2008)</a>	Redshift-evolution: <a href="#">Maiolino et al. (2008)</a>
$Z_g$	Initial gas-phase metallicity	0.25 dex larger than $Z_*$	Offset from $Z_*$ given by difference between $Z_{\text{LW}}$ and $Z_{\text{MW}}$ for star-forming galaxies from this work
$z_q$	Redshift when the star-forming progenitor began quenching through starvation (i.e. when the accretion of gas is halted)	Given by the mass-weighted age of local passive galaxies from this work	Given by the mass-weighted age difference between local green valley and star-forming galaxies from this work
$t_{\text{quench}}$	Duration of quenching (i.e. how long a star-forming progenitor must quench before its stellar metallicity is equal to the stellar metallicity of local passive/green valley galaxies)	Given by the time elapsed since the onset of quenching when $Z_{*,\text{model}} = Z_{*,\text{passive}}$	Given by the time elapsed since the onset of quenching when $Z_{*,\text{model}} = Z_{*,\text{green valley}}$
		Represents the time required to complete quenching	Represents the time elapsed since the onset of quenching (since green valley galaxies have not yet completely quenched)
$\tau_q$	$e$ -folding time for quenching (i.e. the typical time-scale over which most of the star formation and metal enrichment takes place)	Using equation (13), together with the $\lambda_{\text{eff}}$ required to simultaneously reproduce the observed $Z_*$ and SFR in local passive galaxies	Using equation (13), together with the $\lambda_{\text{eff}}$ required to simultaneously reproduce the observed $Z_*$ and SFR in local green valley galaxies



Observational and theoretical studies have shown that there is typically a 0.2–0.3 dex difference between the gas-phase metallicity and stellar metallicity in star-forming galaxies at higher redshift (e.g. Finlator & Dave 2008; Hallday et al. 2008; Peng & Maiolino 2014b; Pipino et al. 2014; Lian et al. 2018c). This result seems to apply across a broad range in stellar mass and in redshift. Hence we set the initial gas metallicity to be 0.25 dex larger than the initial mass-weighted stellar metallicity in our models studying the quenching of star formation within the high- $z$  progenitors of local passive galaxies. On the other hand, studies of star-forming galaxies in the local Universe have shown that the difference between the gas-phase metallicity and stellar metallicity depends quite strongly on stellar mass, with the offset in metallicity decreasing with increasing stellar mass (e.g. González Delgado et al. 2014; Lian et al. 2018a,b). Therefore, in our models studying the quenching of star formation in green valley galaxies in the local Universe, we derive the mass-dependent metallicity offset between gas and stars as given by the difference between the light-weighted stellar metallicity (which traces the gas metallicity) and mass-weighted stellar metallicity for the local star-forming galaxies in our sample, using the light and mass-weighted stellar metallicities provided by FIREFLY.

For local descendants (i.e. passive or green valley galaxies) of stellar mass  $M_*$ , we make the simplifying assumption that their progenitors also had a stellar mass  $M_*$  at the onset of quenching. The initial state  $[g, \epsilon, Z_g, Z_*]$  of a star-forming progenitor of stellar mass  $M_*$  that begins quenching at  $z_q$  is then given by evaluating the scaling relations discussed above at  $(M_*, z_q)$ . A summary of the initial conditions and other important quantities used in our gas regulator model is provided in Table 1.

## 5 PRIMARY QUENCHING MECHANISM

In this section we compare the observed differences in stellar metallicity between star-forming and passive (or green valley) galaxies with the predictions from gas regulator models to put constraints on the nature of the primary quenching mechanism. We will investigate closed-box models, where galaxies quench purely through starvation and with no outflows ( $\lambda_{\text{eff}} = 0$ ), but will also consider leaky-box models, where galaxies quench through a combination of starvation and outflows ( $\lambda_{\text{eff}} > 0$ ). This will allow us to study how the primary quenching mechanism and its associated quenching time-scale depends on stellar mass. On the one hand, we will study how the star-forming progenitors of local passive galaxies quenched, providing insights into the processes responsible for shutting down star formation at high redshift ( $z \sim 1$ –2). On the other hand, we will also address the quenching of star formation in the local Universe, by studying local green valley galaxies that are currently in the process of quenching. Combined, these two studies enable us to probe the evolution of galaxy quenching across cosmic time.

### 5.1 Passive galaxies (quenching at high- $z$ )

We begin by investigating the processes responsible for quenching the star-forming progenitors of local passive

galaxies. Since these passive systems stopped forming stars early on in cosmic history, our analysis in this subsection addresses the quenching of star formation at high redshift. We focus on reproducing the observed stellar metallicity differences  $\Delta Z_*$  between star-forming and passive galaxies with our models. The observed  $\Delta Z_*$  that we will use in the subsequent analysis corresponds to the stellar metallicity difference between local passive galaxies and their star-forming progenitors at high redshift, rather than the observed  $\Delta Z_*$  between local passive galaxies and local star-forming galaxies. It should be noted that our approach is different to what was done in P15, who instead analysed the observed  $\Delta Z_*$  between local passive galaxies and local star-forming galaxies. As was discussed in Section 4.3, the stellar metallicities of the star-forming progenitors are estimated by evolving the stellar metallicities of local star-forming galaxies to higher redshift using the cosmic evolution of the mass-metallicity relation described by Maiolino et al. (2008). The observed stellar metallicities of local passive galaxies and our estimates for the stellar metallicities of their star-forming progenitors are shown in Fig. 5. Since star-forming galaxies at higher redshift are less metal-rich than their local counterparts, the observed stellar metallicity differences between local passive galaxies and their progenitors that are studied in this section are even larger than the metallicity differences between local passive and local star-forming galaxies seen in Fig. 2.

#### 5.1.1 Pure starvation

We first consider closed-box models for galaxy evolution, where galaxies quench purely through starvation and no outflows are included ( $\lambda_{\text{eff}} = 0$ ). A comparison between the observed and model-predicted stellar metallicity differences is shown in the top panel of Fig. 6. The observed stellar metallicity difference between star-forming and passive galaxies is given by the black curve. The model-predicted stellar metallicity enhancements at various times  $\Delta t$  after the onset of quenching are given by the coloured curves. The stellar metallicity enhancements grow with time as successively more metal-rich stars form out of the ISM, which increases the average mass-weighted stellar metallicity of the galaxy. Our models predict that the rate of stellar metallicity enrichment ( $\Delta \log Z_*/\Delta t$ ) decreases with increasing mass, where the change in stellar metallicity in a given time step is smallest for the most massive galaxies. This is primarily because gas fractions decrease with increasing stellar mass, so the most massive galaxies have the smallest gas fractions. As a result, these massive galaxies form relatively fewer new stars compared to the population of stars already present, and so their stellar metallicity increases more slowly.

From Fig. 6, we see that closed-box models are easily able to reproduce the observed stellar metallicity differences. The models typically take about 2 Gyr to reach the level of chemical enrichment seen in local passive galaxies, which suggests that the progenitors of local passive galaxies up to  $M_* \sim 10^{11.2} M_\odot$  that quenched purely through starvation did so over a 2 Gyr time-scale. We study this mass-dependence of the quenching time-scale in more detail in the bottom panel of Fig. 6. We define the quenching time-scale  $t_{\text{quench}}$  as the time-scale over which a galaxy quenching through starvation enriches in stellar metallicity by an amount equal to the

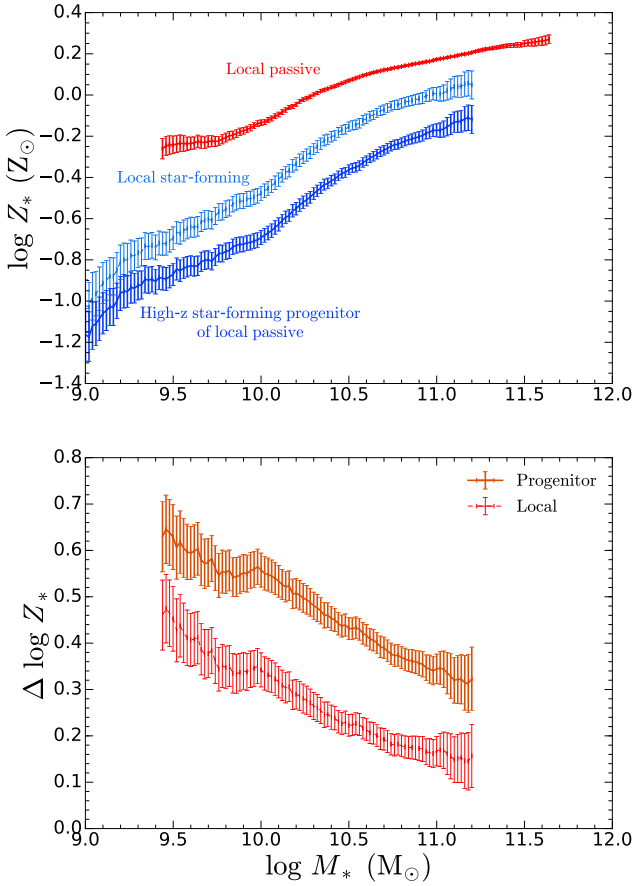


**Figure 5.** Top panel: The stellar mass–stellar metallicity relation observed for local passive galaxies (red) and local star-forming galaxies (light blue), as well as our estimates for the stellar metallicities for the star-forming progenitors of local passive galaxies (dark blue). Bottom panel: The observed difference in stellar metallicity between local star-forming and local passive galaxies (red) and the estimated difference in stellar metallicity between local passive galaxies and their star-forming progenitors at higher redshift (orange).

observed stellar metallicity difference between star-forming and passive galaxies. In other words,  $t_{\text{quench}}$  is the time when our model-predicted enrichment equals the observed stellar metallicity difference. We find that the quenching time-scale is roughly mass-independent and has a typical value of 2 Gyr. Thomas et al. (2010) measured the  $\alpha$ -enhancements in local early-type galaxies and used this information to put constraints on the typical time-scale over which the progenitors of these local passive galaxies formed the bulk of their stars. They find that the progenitors of more massive galaxies formed most of their stars at earlier epochs and over shorter time-scales than their less massive counterparts. At the high-mass end ( $\sim M_* > 10^{10.8}$ ), we find that this quenching time-scale of 2 Gyr is broadly consistent with the star formation time-scales in Thomas et al. (2010). However, at the low-mass end, we find that our quenching time-scales are shorter than the star formation time-scales Thomas et al. (2010). This result might indicate that the progenitors of lower-mass passive galaxies spent a relatively larger fraction of their star-forming lifetime on the main sequence before entering the 2 Gyr quenching phase. Alternatively, our re-

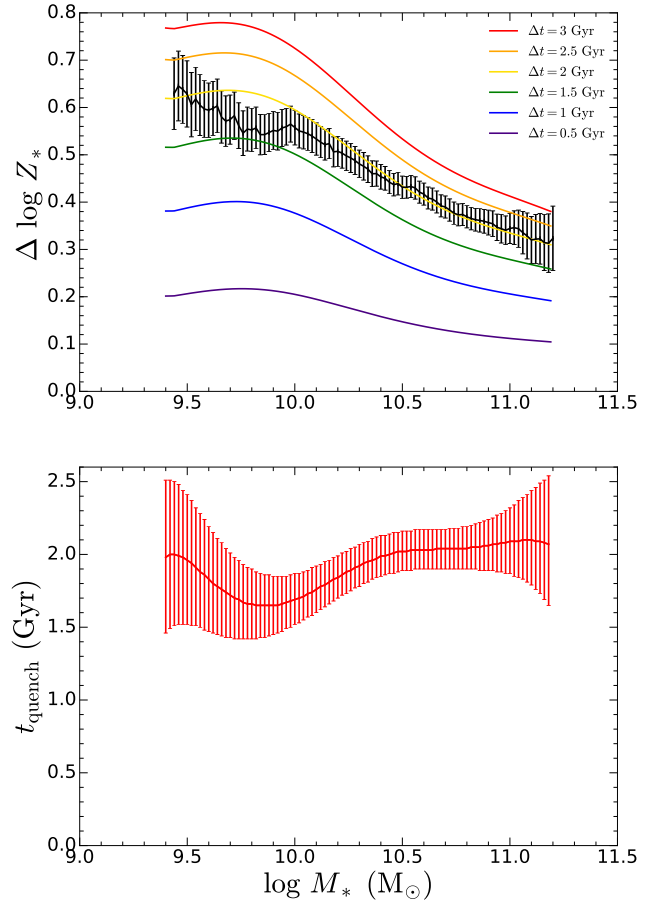


**Figure 6.** Top panel: The observed stellar metallicity difference between local passive galaxies and their star-forming progenitors is shown in black. The coloured lines show the stellar metallicity difference predicted by a closed-box model ( $\lambda_{\text{eff}} = 0$ ) at different times after the onset of starvation. Bottom panel: Quenching time-scales derived from the stellar metallicity difference between star-forming and passive galaxies. The error bars on the quenching time-scales are due to the  $1\sigma$  errors on the stellar metallicity differences.

sults could suggest that the progenitors of low-mass passive galaxies did not quench purely through starvation. We explore alternative scenarios, where galaxies quench through a combination of starvation and outflows later in this section.

We note that the quenching time-scales of 2 Gyr that we obtain are considerably smaller than the 4 Gyr that was found by P15. There are a number of reasons for this. Briefly, on the observational side, we use a different set of stellar metallicities to the original work, which are also mass-weighted rather than light-weighted. On the modelling side, we utilise different scaling relations to specify the initial conditions of the star-forming progenitors in our model, as well as an alternative method to estimate the cosmic epoch when these progenitors begin quenching. In addition, we also distinguish between quenching time-scale  $t_{\text{quench}}$  and epoch of the quenching onset  $z_q$ . In our model, the quenching time-scale refers to the time required for a galaxy to complete quenching, i.e. our findings suggest that galaxies quench purely through starvation for 2 Gyr, at which point quenching has completed. On the other hand, in P15, the quenching

time-scale refers to the amount of time that has elapsed since the onset of quenching through starvation, i.e. their results suggest that we are typically seeing passive galaxies 4 Gyr after the onset of quenching through starvation.

P15 also compared their time-scale of 4 Gyr from the stellar metallicity analysis with the difference in stellar age  $\Delta\text{age}$  between star-forming and passive galaxies. If one assumes that a negligible amount of stars are formed (i.e. passive evolution) during the starvation phase, then this stellar age difference represents the time elapsed since the onset of quenching (which is exactly what  $t_{\text{quench}}$  measures in the P15 model). They find this age difference to be mass-independent at  $\sim 4$  Gyr, which is consistent with the time-scale that was obtained from the stellar metallicity difference analysis. We do not make this comparison between  $t_{\text{quench}}$  and  $\Delta\text{age}$  for passive galaxies in our work. This is because our  $t_{\text{quench}}$  measures the time-scale required to complete quenching, whereas  $\Delta\text{age}$  measures the time elapsed since the onset of quenching, so these two quantities trace different time-scales and are therefore not comparable. To clarify, after a galaxy completes quenching (i.e. it becomes passive),  $t_{\text{quench}}$  remains fixed, but its  $\Delta\text{age}$  continues to increase indefinitely as more time elapses, and so these two quantities begin to diverge. We note that we will make a comparison between  $t_{\text{quench}}$  and  $\Delta\text{age}$  for green valley galaxies in Section 5.2. Unlike passive galaxies, green valley galaxies are still in the process of quenching and so  $t_{\text{quench}}$  actually measures the time since the onset of quenching (rather than the time to complete quenching), so a meaningful comparison between  $t_{\text{quench}}$  and  $\Delta\text{age}$  can be made.

Our closed-box model suggests that the progenitors of local passive galaxies quenched through starvation for 2 Gyr, as that is the time required to reproduce the observed stellar metallicity differences. However, we can see from Fig. 6 that the model-predicted curves can exceed the observed stellar metallicity differences, as they continue to grow even after 2 Gyr of quenching through starvation has elapsed. There is clearly still a substantial increase in the stellar metallicity enhancement  $\Delta Z_*$  during the subsequent timesteps  $\Delta t$  after the observed stellar metallicity difference has been reached. If these galaxies were actually quenched, then there should only be a residual amount of chemical enrichment after 2 Gyr as all the gas has been exhausted, and there is only a marginal amount of star formation remaining. The ‘quenched’ galaxies in our closed-box model still have a relatively large gas reservoir and are still forming a considerable number of stars. This is in contrast with the observed properties of local passive galaxies, which have small gas reservoirs and are not actively forming stars. Furthermore, since the ‘quenched’ galaxies in our model continue to form stars and become progressively more enriched, their stellar metallicities begin to exceed the stellar metallicities seen in local passive galaxies, as shown by the top panel in Fig. 6.

In order to prevent this prolonged chemical enrichment in our closed-box model, an additional mechanism must kick in, when the observed stellar metallicity difference has been reached ( $\sim 2$  Gyr), which abruptly stops any further star formation and enrichment. This mechanism could be some form of an ejective mode or heating mode that starts to play a role near the end of the starvation phase, to prevent further chemical enrichment from taking place. There are a number of mechanisms that could eject the remaining gas in

the galaxy at the end of the starvation phase. For example, an AGN that is being activated could clear or heat the gas (e.g. Ciotti & Ostriker 2007; Ciotti et al. 2009). Satellite galaxies plunging through the hot ICM could rapidly lose their gas through ram pressure stripping, and this may happen only when the galaxy enters deep into the cluster (Muzzin et al. 2014). Alternatively, the integrated feedback from many Type Ia supernovae could eject or heat the remaining gas (Pipino & Matteucci 2004; Matteucci et al. 2006; Pipino & Matteucci 2006; Pipino et al. 2008). Since supernovae are more effective at driving away material in low density conditions, this mechanism is especially effective at ejecting gas at the end of the starvation phase, when the gas content has diminished and the densities have fallen. Moreover, type Ia SNe have a well defined time-scale ( $\sim 1$ – $2$  Gyr) before they start contributing significantly to the energy injection into the ISM, which would explain well why the additional ejective/heating mode kicks in only around 2 Gyr after the last episode of major star formation, i.e. after the onset of quenching.

To summarise, our closed-box model suggests that the progenitors of local passive galaxies quenched purely through starvation over a time-scale of 2 Gyr, and then additional star formation and additional chemical enrichment was abruptly halted by the onset of an ejective or heating mode. However, as an alternative, our results may also suggest that the progenitors of local passive galaxies did not quench purely through starvation. Indeed, other models, such as a combination of starvation and outflows during the quenching, may potentially provide a better description of the quenching process as discussed in the following sections.

### 5.1.2 Starvation with outflows

We now study leaky-box models for galaxy evolution, where galaxies quench through a combination of starvation and outflows. In this section we assume  $\lambda_{\text{eff}} = 1$ . Our results are shown in Fig. 7. The main effect of introducing outflows in our model is that the gas reservoir depletes faster than in the closed-box case, as now both star formation and galactic winds drain the gas content. This has two main consequences for our model predictions. Firstly, since the gas reservoir depletes more rapidly, the star formation rate also declines faster and less stars are formed within a given time interval. As a result, the stellar metallicity increases more slowly in the leaky-box model. Hence any quenching time-scales we derive in our analysis (i.e. the time derived to match  $\Delta Z_*$ ) will be longer than in the closed-box model. Secondly, only a fraction of the initial gas reservoir is now converted into new, metal-rich stars. The rest of the gas is expelled, so the amount of material that is actually available to increase the stellar metallicity of the galaxy has been reduced. As a result, the maximum stellar metallicity increase of the galaxy, which occurs when the gas reservoir is completely depleted, is lower in the leaky-box models. Hence it may become more difficult for our model to reproduce the stellar metallicity differences that have been observed.

We find that models incorporating outflows are also capable of reproducing the observed stellar metallicity differences seen in low-mass galaxies, with  $\log(M_*/M_\odot) < 10.0$ . These low-mass systems have sufficiently large gas fractions

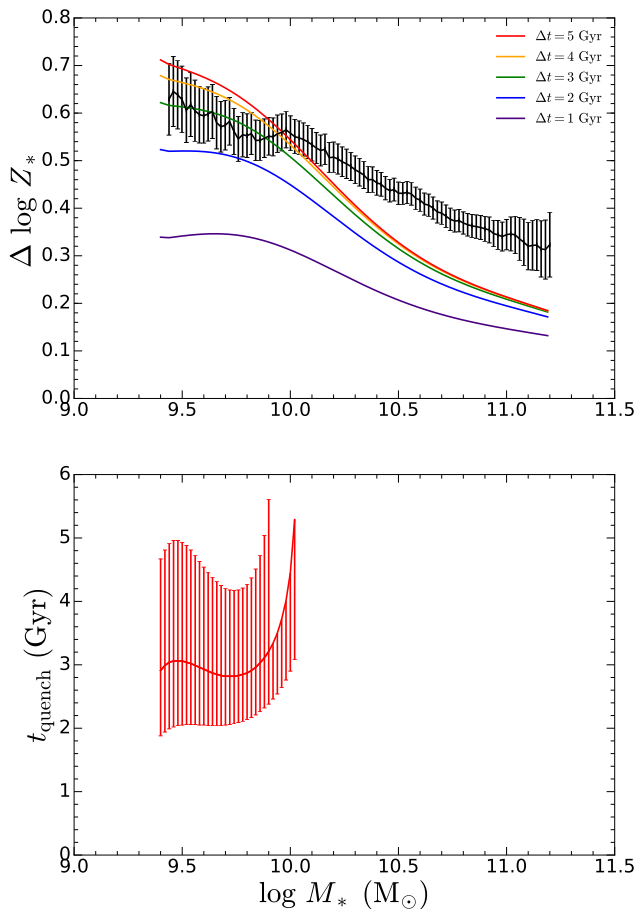


**Figure 7.** Similar to Fig. 6, but we now consider a leaky-box model, incorporating outflows with  $\lambda_{\text{eff}} = 1$ . Also note that the timesteps in our model are now 1 Gyr (instead of the 0.5 Gyr used in Fig. 6). In the cases when the upper limit on the stellar metallicity difference  $\Delta Z_*$  cannot be reproduced by our model, only the lower limit on the quenching time-scale  $t_{\text{quench}}$  is shown.

so that the observed stellar metallicity enhancement can be achieved, even if a substantial amount of gas is removed by outflows. Due to the reduced rate of chemical enrichment caused by the removal of gas, the typical quenching time-scales are longer than those found with the closed-box model. In the specific case of  $\lambda_{\text{eff}} = 1$ , the bottom panel of Fig. 7 shows that the typical quenching time-scale is between 3–4 Gyr for galaxies with  $\log(M_*/M_\odot) < 10.0$ . Since both closed-box models (pure starvation) and leaky-box models (starvation with outflows) are consistent with the observations, we conclude that outflows could have potentially played an important role in shutting down the star formation in the progenitors of low-mass passive galaxies. Lian et al. (2018a,b) also find that outflows could potentially be more important in driving evolution in low-mass galaxies, as they show that either strong, time-dependent outflows with large metal-loading factors, or a time-varying IMF must be invoked to simultaneously reproduce both the gas MZR and the stellar MZR in local low-mass star-forming galaxies.

On the other hand, the predictions from our leaky-box model are inconsistent with the stellar metallicity differences observed in high-mass galaxies with  $\log(M_*/M_\odot) > 10.0$ . Outflows with  $\lambda_{\text{eff}} = 1$  remove too much gas in these

massive systems, preventing sufficient chemical enrichment during quenching. Our findings suggest that powerful outflows played a minor role in quenching the progenitors of high-mass passive galaxies. These massive galaxies either quenched purely through starvation for 2 Gyr before any future star formation was abruptly halted by the onset of an ejective or heating mode, or through a combination of starvation and weak outflows, with  $\lambda_{\text{eff}} < 1$ . Note, that this does not mean that outflows are not present in massive galaxies, but that most of the outflowing gas does not escape and is being recycled (i.e. the ‘classical’ loading factor can be  $\lambda \sim 1$  even if  $\lambda_{\text{eff}} < 1$ ).

### 5.1.3 Further constraints on quenching

Until now, we have only been using the observed stellar metallicity differences to put constraints on the nature of quenching. We have investigated whether given models can reproduce the observed stellar metallicity enhancement and we have determined the time-scale required to achieve this. So far we have only been considering models consisting of pure starvation ( $\lambda_{\text{eff}} = 0$ ) and models incorporating a combination of starvation and outflows ( $\lambda_{\text{eff}} = 1$ ). As we have seen, increasing  $\lambda_{\text{eff}}$  decreases the rate of stellar metallicity enrichment and lengthens the time-scale required to reproduce the observed  $\Delta Z_*$ . At any mass, if  $\lambda_{\text{eff}}$  is set too large, outflows become too prominent and remove a significant fraction of the available gas, rendering it impossible to enrich by  $\Delta Z_*$ . Therefore, there are a range of  $\lambda_{\text{eff}}$  values that can reproduce the observed stellar metallicity differences, each with different quenching time-scales. Hence there is a level of degeneracy in our analysis, as the quenching time-scale that is derived depends on the value of  $\lambda_{\text{eff}}$  that is assumed.

A further, important constraint that should help break the  $\lambda_{\text{eff}} - t_{\text{quench}}$  degeneracy comes from analysing the star formation rates of these galaxies that are being quenched. At the moment when  $\Delta Z_*$  enrichment is achieved, our model galaxy has a stellar metallicity that is comparable to that of local passive galaxies. In principle this galaxy should therefore also have a star formation rate that is consistent with those of local passive galaxies. However, as was found in 5.1.1, the ‘quenched’ galaxies in our  $\lambda_{\text{eff}} = 0$  model still had a non-negligible star formation rate. Rather than invoking a second, abrupt quenching phase (as was done in Section 5.1.1), we aim, in this subsection, to simultaneously reproduce both the observed stellar metallicity and the star formation rate in local passive galaxies, using a time-independent mass loading factor  $\lambda_{\text{eff}}$ . We require that when the galaxy’s stellar metallicity enrichment equals the observed stellar metallicity difference  $\Delta Z_*$ , its current SFR and  $M_*$  place it in the passive region of the SFR- $M_*$  plane in Fig. 1. Since galaxies that quench with different  $\lambda_{\text{eff}}$  values will have different star formation rates at the moment  $\Delta Z_*$  enrichment is satisfied, if  $\lambda_{\text{eff}}$  is chosen to be too small, then the star formation rate will still be too large. On the other hand, if  $\lambda_{\text{eff}}$  is too large, then too much gas is removed and it is impossible for the galaxy to ever satisfy the enrichment criterion. Hence there will only be a range of  $\lambda_{\text{eff}}$  values that can simultaneously reproduce both the observed stellar metallicity and star formation rate in local passive galaxies.

We show the quenching time-scales derived from our



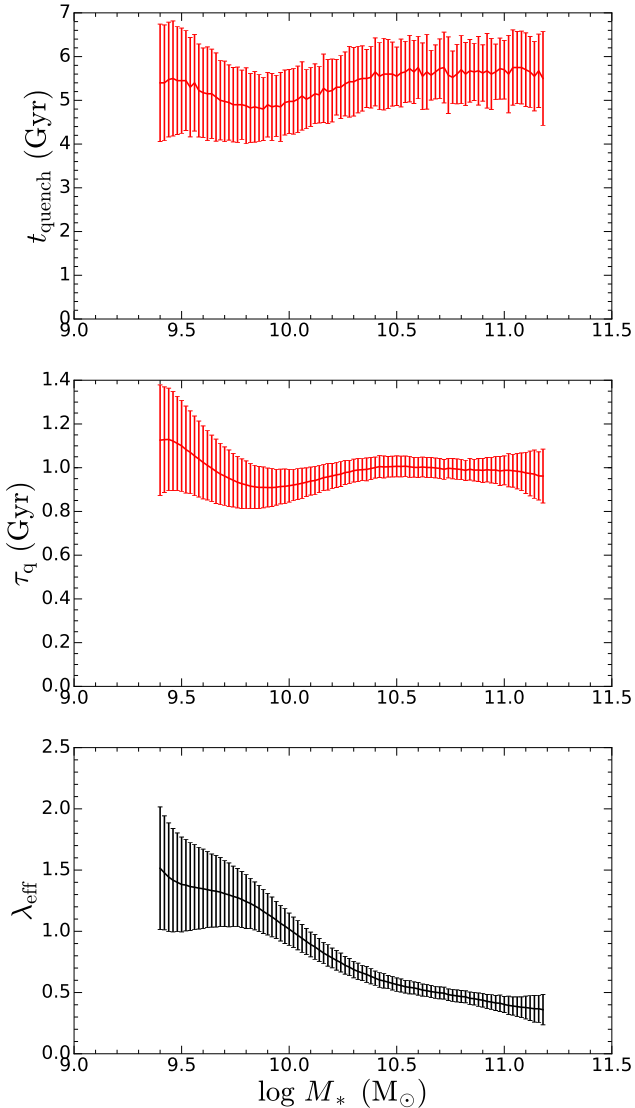


**Figure 8.** Top panel: Similar to the bottom panel in Fig. 6, but we now apply our joint metallicity-SFR analysis. Middle panel: The  $e$ -folding time-scales  $\tau_q$ , which indicate the typical time-scale over which the star formation rate declines and the stellar metallicity enriches, as a function of stellar mass. Bottom panel: The mass-loading factors  $\lambda_{\text{eff}}$  required to simultaneously satisfy the  $\Delta Z_*$  and the SFR quenching criteria. We show the median  $e$ -folding time-scale and mass-loading factor in each stellar mass bin, with the error bars representing the standard deviation.

joint metallicity-SFR analysis in the top panel of Fig. 8. We find that the typical quenching time-scale is essentially mass-independent at  $\sim 5.5$  Gyr, which is considerably larger than the time-scales we found in the  $\lambda_{\text{eff}} = 0$  and  $\lambda_{\text{eff}} = 1$  scenarios. In particular, the predicted quenching time-scales for massive galaxies with  $M_* > 10^{11} M_\odot$  are much longer than the estimates obtained from the analysis of  $\alpha$ -enhancements (Thomas et al. 2010). This suggests that models combining starvation with continuous outflows provide a poor description for the quenching of the progenitors of massive passive galaxies. Therefore at the high-mass end, our closed-box models, where galaxies quench purely through starvation for 2 Gyr before a sudden ejective/heating mode halts fu-

ture star formation, are preferred as the predicted quenching time-scales are shorter. However, we do note that this tension at the high-mass end between the quenching time-scales derived from our model with starvation and continuous outflows and the estimates obtained from  $\alpha$ -enhancements is somewhat reduced when we instead look at the typical  $e$ -folding time-scale during the quenching phase. As shown by the model-predicted curves in the top panel of Fig. 7, the stellar metallicity initially increases quite rapidly, but quickly slows down as it asymptotically approaches its limiting value. Hence, although the duration of quenching  $t_{\text{quench}}$  is long (top panel of Fig. 8), the typical time-scale  $\tau_q$  over which the stellar metallicity increases is considerably shorter ( $\sim 1$  Gyr), which we show in the middle panel of Fig. 8. In our models, the star formation rate declines exponentially according to

$$\Psi(t) = \Psi_0 e^{-t/\tau_q}, \quad (12)$$

as gas is converted into stars and removed in galactic winds. Therefore,  $\tau_q$  represents the  $e$ -folding time-scale over which the star formation rate decreases by a factor of  $e$ , and is given by

$$\tau_q = \frac{1}{\epsilon(1 - R + \lambda_{\text{eff}})}. \quad (13)$$

Although the star formation efficiency  $\epsilon$  and the ‘effective’ mass-loading factor  $\lambda_{\text{eff}}$  depend on stellar mass (see bottom panel), we find that  $\tau_q$  is mostly mass-independent. Since  $\tau_q$  is an  $e$ -folding time-scale, the bulk of the stellar metallicity enrichment occurs within the earlier stages of the quenching phase, over a time-scale of roughly  $2-3 \tau_q$ , which is substantially shorter than the total duration  $t_{\text{quench}}$  of the quenching phase.

We show the mass-loading factors required to simultaneously reproduce the stellar metallicity and SFR of passive galaxies in the bottom panel of Fig. 8. We find that the mass-loading factor strongly decreases with increasing stellar mass. This indicates that ‘effective’ outflows (which are capable of permanently removing gas from the galaxy) are, together with starvation, of increasing importance in low-mass galaxies, where we find that galaxies with  $M_* < 10^{10} M_\odot$  typically have  $\lambda_{\text{eff}} \geq 1$ . On the other hand, outflows play a more minor role in quenching massive galaxies, as galaxies with  $M_* > 10^{10.5} M_\odot$  typically have  $\lambda_{\text{eff}} \leq 0.5$ . Although these massive galaxies may be ejecting large amounts of gas in the form of outflows (i.e. a large  $\lambda$ ), our results suggest that most of the outflowing gas does not escape the galaxy and is instead recycled (i.e. a small  $\lambda_{\text{eff}}$ ). The anti-correlation between stellar mass and  $\lambda_{\text{eff}}$  that we find is broadly consistent with the mass dependence in theoretical models, which predict that  $\lambda \propto M_*^{-1/3}$  (Murray et al. 2005) for momentum-driven winds and  $\lambda \propto M_*^{-2/3}$  for energy-driven winds (e.g. Dekel & Silk 1986), as well as other observational evidence (e.g. Heckman et al. 2015; Chisholm et al. 2017; Fluetsch et al. 2018).

As was shown this subsection, our models can simultaneously match the stellar metallicity and star formation rate observed in local passive galaxies by considering the starvation with outflows scenario and finding the appropriate ‘effective’ mass-loading factor  $\lambda_{\text{eff}}$ . In addition, in Section 5.1.1, we explored the pure starvation scenario ( $\lambda_{\text{eff}} = 0$ ) and found that an ejective or heating mode that kicks in

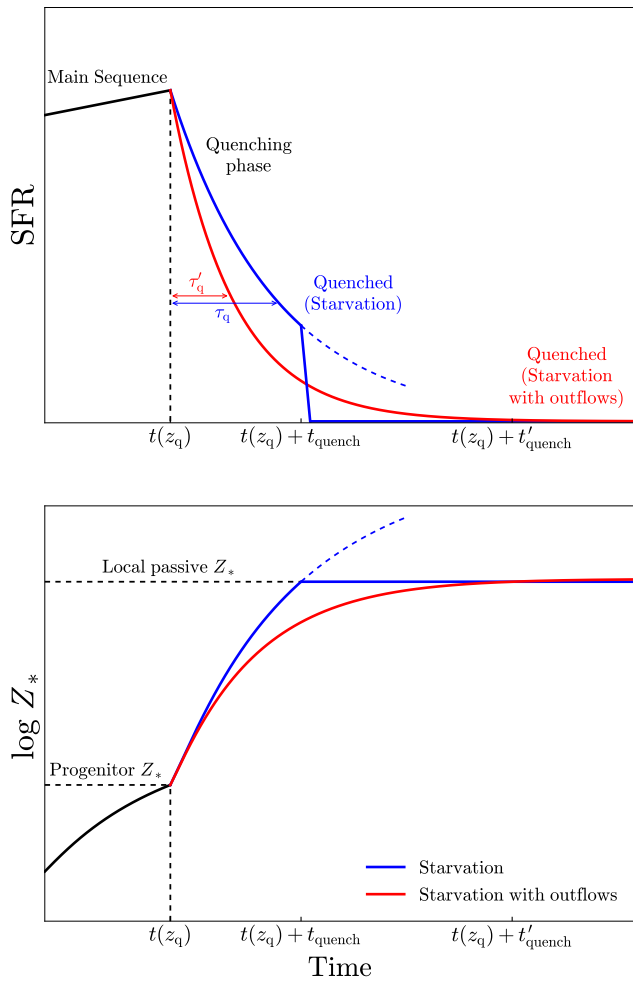


**Figure 9.** A schematic illustration of the evolution of the star formation rate (SFR, top panel) and the evolution of the logarithmic stellar metallicity ( $\log Z_*$ , bottom panel) during the quenching phase in our models. The galaxy initially evolves along the star-forming main sequence. At a time  $t(z_q)$ , the accretion of cold gas is halted and the galaxy begins quenching through starvation ( $\lambda_{\text{eff}} = 0$ , blue) or through starvation with outflows ( $\lambda_{\text{eff}} > 0$ , red). In the starvation scenario, the galaxy quenches for a time-scale  $t_{\text{quench}}$  before it reaches the level of chemical enrichment seen in local passive galaxies, at which point the onset of an ejective or heating mode prevents any further star formation and chemical enrichment, and the galaxy is quenched. In the starvation with outflows scenario, after a time  $t'_{\text{quench}}$  has elapsed the galaxy has completed quenching, and both its stellar metallicity and star formation rate are similar to that seen in local passive galaxies.  $\tau_q$  and  $\tau'_q$  represent the  $e$ -folding time-scales in the starvation, and starvation with outflows scenarios, respectively.

at the end of the quenching phase had to be invoked in order to match the observed stellar metallicity and SFR of passive galaxies. We schematically show the evolution of the star formation rate and the evolution of the logarithmic stellar metallicity during the quenching phase in both of these models in Fig. 9. The main aspects of these two quenching models is summarised in the following. Prior to the onset of quenching, the galaxy evolves along the star-forming main sequence, where its gas reservoir is in quasistatic equilibrium, so the star formation rate increases slowly, and the

stellar metallicity increase is modest due to dilution by accretion of pristine gas. At a time  $t(z_q)$ , the accretion of cold gas is halted and the galaxy begins quenching through starvation. The blue curve shows the evolution in the case of pure starvation ( $\lambda_{\text{eff}} = 0$ ) that was explored in Section 5.1.1, while the red curve shows the evolution in the case of starvation with outflows ( $\lambda_{\text{eff}} > 0$ ) which we explored in this subsection. The  $e$ -folding time-scale for the model incorporating outflows  $\tau'_q$  is shorter than for the model including only starvation  $\tau_q$ , as the additional gas that is lost through galactic winds causes the star formation rate to decline more quickly. In the pure starvation scenario, the galaxy quenches for a time-scale  $t_{\text{quench}}$  before it has a stellar metallicity that matches the stellar metallicity observed for a local passive galaxy of the same stellar mass. However, these galaxies still harbour a relatively large gas reservoir, and so continued star formation beyond  $t = t(z_q) + t_{\text{quench}}$  in our model would result in a galaxy that is too metal-rich (as shown by the dashed blue curves). In order to prevent further star formation and chemical enrichment, an ejective or heating mode is required, which completely quenches the galaxy, reducing the star formation rate to zero and keeping the stellar metallicity constant at a fixed value. In the starvation with outflows scenario, the quenching phase has a duration  $t'_{\text{quench}}$ , at which point both the stellar metallicity and the star formation rate of the galaxy in our model are similar to those seen in local passive galaxies of the same stellar mass.

## 5.2 Green valley galaxies (quenching in the local Universe)

We now investigate the processes responsible for quenching star formation in galaxies in the local Universe, by studying the green valley galaxy population, which is currently in the process of quenching. Our analysis is similar to Section 5.1, but we now consider the stellar metallicity difference between star-forming galaxies and green valley galaxies. Since green valley galaxies have only recently begun quenching, the stellar metallicities of their progenitors are only slightly smaller than the stellar metallicities of local star-forming galaxies. Hence the stellar metallicity differences between green valley galaxies and their star-forming progenitors are only slightly larger than the differences seen in Fig. 2.

### 5.2.1 Pure starvation

A comparison between the observed and model-predicted stellar metallicity differences is shown in the top panel of Fig. 10. We find that our closed-box model is able to reproduce the observed stellar metallicity differences, which could potentially suggest that the majority of green valley galaxies are quenching through starvation. Furthermore, the closed-box models typically require 3.5 Gyr of quenching to reach the level of enrichment seen in observations, which implies that we are typically seeing these green valley galaxies 3.5 Gyr after the onset of quenching. These quenching time-scales for local green valley galaxies are longer than the quenching time-scales of  $\sim 2$  Gyr that were found for the progenitors of local passive galaxies in Section 5.1. Coupled with the fact that passive galaxies have completed quenching, while green valley galaxies are still in the process of

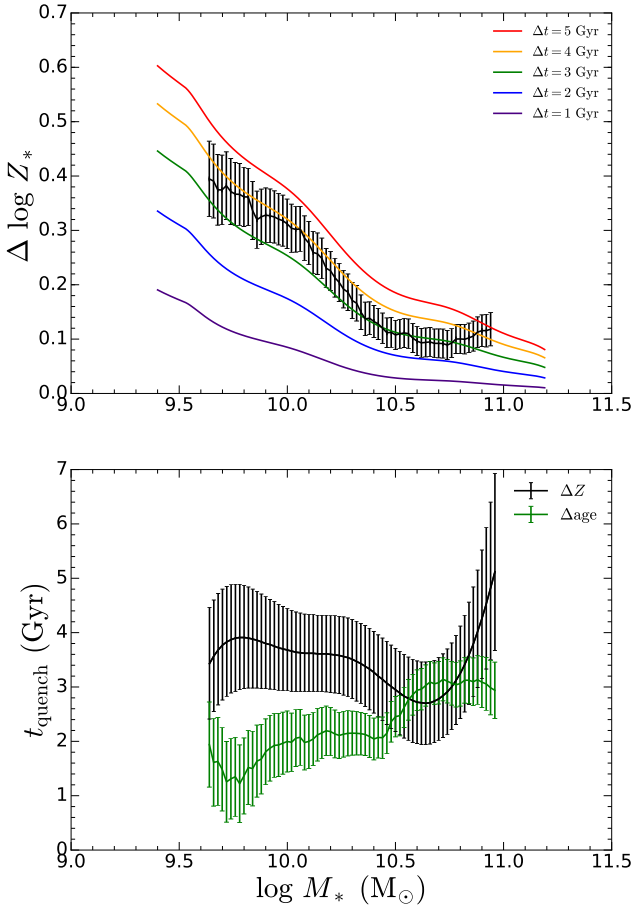


**Figure 10.** Top panel: The observed stellar metallicity difference between star-forming galaxies and green valley galaxies is shown in black. The coloured lines show the stellar metallicity difference predicted by a closed-box model ( $\lambda_{\text{eff}} = 0$ ) at different times after the onset of starvation. Bottom panel: Quenching time-scales derived from the stellar metallicity difference ( $\Delta Z$ ) between star-forming galaxies and green valley galaxies (black), as well as the quenching time-scales obtained from the stellar age difference ( $\Delta \text{age}$ ) between star-forming and green valley galaxies (green). The error bars on the  $\Delta Z$ -derived and  $\Delta \text{age}$ -derived quenching time-scales are due to the  $1\sigma$  errors on the stellar metallicity and stellar age differences, respectively.

quenching (and so would take even longer to fully complete quenching), galaxies in the local Universe must be quenching much more slowly than their counterparts at higher redshift. This increase in quenching time-scale is mostly due to the fact that gas depletion time-scales in the local Universe are longer than at high redshift (e.g. Tacconi et al. 2013; Santini et al. 2014; Genzel et al. 2015; Schinnerer et al. 2016; Scoville et al. 2017; Tacconi et al. 2018), so it takes more time for galaxies to exhaust their gas reservoir during starvation.

The mass-dependence of the quenching time-scale is shown more clearly in the bottom panel of Fig. 10. The quenching time-scale obtained from our stellar metallicity difference analysis is shown by the black curve. We find that the quenching time-scale is roughly between 3–4 Gyr for galaxies with  $\log(M_*/M_\odot) < 10.8$  (i.e. similar to what found by Peng et al. 2015, in their original analysis). Above this mass threshold the quenching time-scale grows strongly with

increasing mass, due to the increase in the observed stellar metallicity difference with increasing stellar mass within this regime. This result may have a physical origin, i.e. starvation is more effective in the high-mass regime, or we may be potentially misclassifying galaxies within this mass range.

We also estimate quenching time-scales from the observed stellar ages of star-forming and green valley galaxies. If we make the simplifying assumption that galaxies evolve passively (i.e. no additional stars are formed) during the quenching phase, then from equation (11) and the discussion that followed, the time since the onset of quenching is just given by the difference in the stellar ages of star-forming and green valley galaxies. These stellar age differences then provide an alternative, independent estimate for the quenching time-scale. The quenching time-scales derived from the stellar age differences ( $\Delta \text{age}$ ) are shown by the green curve in the bottom panel of Fig. 10. The typical stellar age difference between star-forming and green valley galaxies is within 2–3 Gyr, indicating that we are witnessing green valley galaxies roughly 2.5 Gyr after the onset of quenching. We find that the quenching time-scales derived from our stellar metallicity analysis are roughly consistent with the time-scales obtained from the stellar age differences. However, there are some discrepancies between these two estimates which we shall discuss further.

At the low-mass end, with  $\log(M_*/M_\odot) < 10.5$ , the time-scales resulting from the metallicity difference  $\Delta Z$  are systematically larger than the time-scales inferred from the age differences  $\Delta \text{age}$ . This should not be too surprising as we made the simplifying assumption that galaxies evolve passively during quenching. Of course, young, metal-rich stars will be formed during quenching which will increase the average stellar metallicity and also decrease the average stellar age of the galaxy. Hence the observed stellar age of real green valley galaxies, which do not evolve passively, will be smaller than the idealised, passively-evolving green valley galaxies that we were considering. As a result, the age difference between star-forming and green valley galaxies that we observe will be smaller than the actual duration of quenching. In other words, the quenching time-scales from our  $\Delta \text{age}$  analysis are likely underestimated. This effect is strongest at the low-mass end, where galaxies have larger gas fractions and form relatively more stars during the starvation phase. This explains why we found the  $\Delta Z$  time-scales to be consistently larger than the  $\Delta \text{age}$  time-scales at the low-mass end.

Numerous works have also studied the typical time-scales over which galaxies in the local Universe quench. For example, Wetzel et al. (2013) and Fossati et al. (2017) used N-body simulations/semi-analytic models to track satellite orbits, and subsequently determined the quenching time-scales that were needed to match the quenched fraction of local satellite galaxies observed in SDSS DR7. They find that the typical quenching time-scale decreases with increasing mass, with Wetzel et al. (2013) finding the time-scale to decrease from 4 Gyr at  $M_* = 10^{10} M_\odot$  to 2 Gyr at  $M_* = 10^{11} M_\odot$ , while Fossati et al. (2017) find that the time-scale decreases from 8 Gyr at  $M_* = 10^{10} M_\odot$  and 6 Gyr at  $M_* = 10^{11} M_\odot$ . In a similar vein, Guo et al. (2017) also determined estimates for the time-scale upon which satellite galaxies must quench, following accretion into the group/cluster halo. Using dynamical arguments, they find that low-mass ( $9.5 < \log(M_*/M_\odot) < 10.5$ ) galaxies typi-

cally quench over a time-scale of 7 Gyr. As is expected, the quenching time-scales,  $t_{\text{passive}}$ , from these works (except the 2 Gyr from [Wetzel et al. \(2013\)](#)) are larger than the time-scales,  $t_{\text{green}}$ , we derive in our analysis. This should be the case because  $t_{\text{passive}}$  measures the total time required to complete quenching (transforming a galaxy from star-forming to passive), while our time-scales measure the time that green valley galaxies have been quenching for so far. Since green valley galaxies are still in the process of quenching and require additional time to complete the transformation into passive galaxies,  $t_{\text{green}} < t_{\text{passive}}$ .

### 5.2.2 Starvation with outflows

A comparison between the observed stellar metallicity differences and the predictions from models with  $\lambda_{\text{eff}} = 1$  is shown in Fig. 11. We find that models incorporating outflows struggle to reproduce the observed stellar metallicity differences. Furthermore, in cases when the metallicity differences can be reproduced, the quenching time-scales that are derived are inconsistent with the time-scales obtained from the  $\Delta\text{age}$  analysis. These results suggest that powerful outflows play a minor role in quenching star formation in galaxies in the local Universe.

### 5.2.3 Further constraints on quenching

Similar to Section 5.1.3, we determine the range of  $\lambda_{\text{eff}}$  such that both the  $\Delta Z_*$  and the SFR quenching criteria are simultaneously satisfied. This means that when the galaxy's stellar metallicity enrichment in our model equals the observed stellar metallicity difference  $\Delta Z_*$ , its SFR and  $M_*$  place it in the green valley galaxy locus of the SFR- $M_*$  plane in Fig. 1.

The quenching time-scales  $t_{\text{quench}}$  derived from our joint metallicity-SFR analysis are shown in the top panel of Fig. 12. We also show the  $e$ -folding time-scales  $\tau_q$  in the middle panel, and the associated mass-loading factors in the bottom panel. The quenching durations  $t_{\text{quench}}$  are roughly mass-independent at  $\sim 5.5$  Gyr, which is comparable to what was seen for passive galaxies in Fig. 8. As mentioned earlier, since local green valley galaxies are still in the process of quenching, this means that the total time required to complete the quenching phase and fully transition to the passive sequence will be longer than the  $t_{\text{quench}}$  that has been obtained, indicating that local green valley galaxies quench more slowly than their counterparts at higher redshift. This is illustrated more clearly by the  $e$ -folding time-scales  $\tau_q$ , which are roughly mass-independent at  $\sim 2$  Gyr, and are larger than what was obtained in our study of local passive galaxies ( $\sim 1$  Gyr). Furthermore, we find that the mass-loading factors  $\lambda_{\text{eff}}$  tend to be smaller than inferred at high- $z$ , indicating that outflows on average are likely less powerful or less ubiquitous in the local Universe. Similar to our study of passive galaxies, we find that the typical mass-loading factor decreases with increasing mass, indicating that ‘effective’ outflows play an important role for local low-mass galaxies, but become gradually less important at high masses, which implies that the outflowing gas in local massive galaxies does not escape and is instead reaccreted.

However, we do note that the long quenching time-scales  $t_{\text{quench}}$  that we have derived are substantially larger

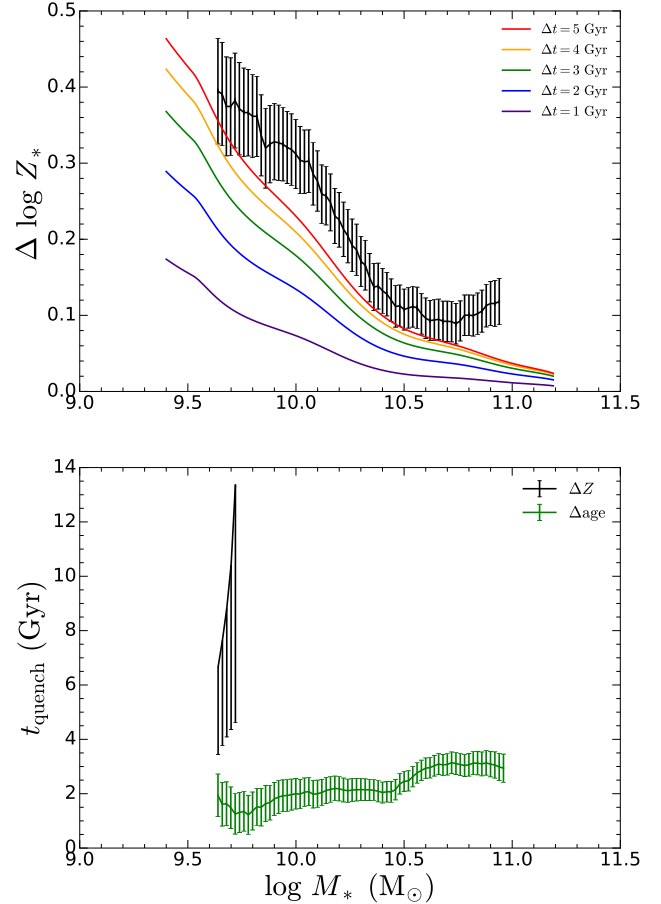


**Figure 11.** Similar to Fig. 10, but we now consider a leaky-box model, incorporating outflows with  $\lambda_{\text{eff}} = 1$ . In the cases when the upper limit on the stellar metallicity difference  $\Delta Z_*$  cannot be reproduced by our model, only the lower limit on the quenching time-scale  $t_{\text{quench}}$  is shown.

than the time-scales obtained from the stellar age difference analysis (Fig. 12), while our  $e$ -folding time-scales  $\tau_q$  are more comparable. This inconsistency between these two estimates for the duration of quenching may be due to the fact that the stellar age difference only provides a very rough estimate for the quenching time-scale, which, as discussed in Section 5.2.1, is in fact an underestimate of the true duration of quenching. It is also possible that our model, which assumes continuous outflows, with a constant, large mass-loading factor does not provide an adequate description of how star formation is shut down in local green valley galaxies. This would suggest that another mechanism, which together with starvation, allows for a significant increase in stellar metallicity together with a rapid reduction in the star formation rate.

Alternatively, and perhaps more likely, the inconsistency between quenching time-scale inferred from the metallicities and the age differences observed in Fig. 12, may reflect the limits of the dataset. Indeed, the Sloan fibre only probes the central region of galaxies. While this is not a major problem for star-forming galaxies and passive galaxies (which have mild metallicity and age gradients, [Belfiore et al. 2017a](#); [Goddard et al. 2017a](#)) it is a potential issue for green valley galaxies, which often have a quenched cen-



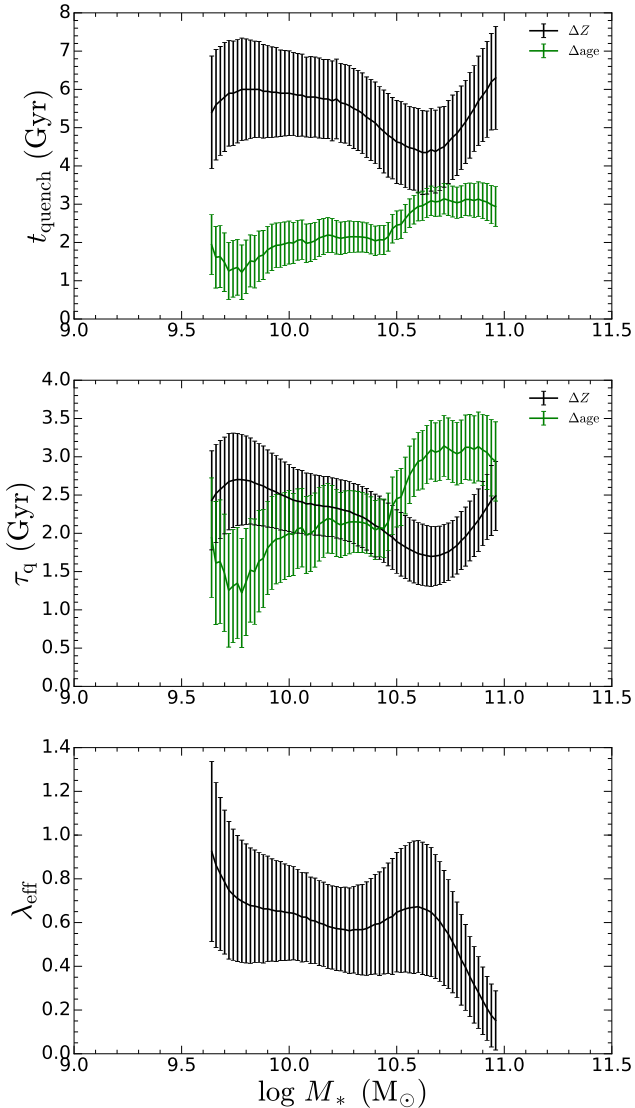


**Figure 12.** Top panel: Similar to the bottom panel in Fig. 10, but we now apply our joint metallicity-SFR analysis. Middle panel: The  $e$ -folding time-scales  $\tau_q$ , which indicate the typical time-scale over which the star formation rate declines and the stellar metallicity enriches, as a function of stellar mass. Bottom panel: The mass-loading factors  $\lambda_{\text{eff}}$  required to simultaneously satisfy the  $\Delta Z_*$  and the SFR quenching criteria. We show the median  $e$ -folding time-scale and mass-loading factor in each stellar mass bin, with the error bars representing the standard deviation.

tral region and an outer (much younger) star-forming disc (Belfiore et al. 2017b, 2018). The physical properties in green valley galaxies that vary rapidly with galactocentric radius are not properly probed by the single-fibre SDSS data, and may likely introduce some inconsistencies in our analysis. It will be possible to further investigate the quenching of green valley galaxies, overcoming the limitations of a single fibre, by analysing the spatially-resolved spectral data provided by integral field spectroscopic galaxy surveys, such as SDSS-MaNGA (although at the expense of statistics).

## 6 ENVIRONMENTAL EFFECTS

In this section we will discuss how galaxy quenching, as probed by the stellar metallicity difference between star-forming and passive (or green valley) galaxies, depends on the environment. This will allow us to determine whether there is an environmental origin for starvation, allowing us to put constraints on the nature of the starvation mechanism. We will firstly investigate if there are any differences in the way that central galaxies and satellite galaxies quench. We will then study environmental quenching in more detail by investigating the dependence of galaxy quenching on the local overdensity.

It should be noted that we compare the difference in stellar metallicity between local star-forming galaxies and local passive (or green valley) galaxies in this section, rather than the stellar metallicity difference between local passive (or green valley) galaxies and their star-forming progenitors, as was done in Section 5. This was done in order to avoid the issue of determining the stellar metallicity and quenching epoch  $z_q$  of the star-forming progenitors, which may depend on environment, and so in principle could be different for centrals and satellites, as well as for galaxies residing in different local overdensities. Indeed, studies have shown that the metal content in galaxies is sensitive to the local environment. For instance, Peng & Maiolino (2014a) found that star-forming satellites in denser environments tend to have larger gas-phase metallicities. Furthermore, the quenching epoch could be dependent on environment, as various studies have found evidence suggesting that galaxy formation in low-density environments occurs at later epochs (e.g. Kuntschner et al. 2002; Terlevich & Forbes 2002; Thomas et al. 2005). However, this scenario is not yet completely established, as other studies, such as Thomas et al. (2010) find that both the galaxy formation epoch as well as the typical formation time-scale are independent of environment.

### 6.1 Central–satellite dichotomy

We use our central–satellite classification scheme to divide our sample of SDSS galaxies into centrals and satellites. After applying the usual cuts in redshift and S/N our sample consists of 37,910 central galaxies and 14,369 satellite galaxies. We then apply our SFR- $M_*$  classification criterion to further divide this sample into star-forming, green valley and passive galaxies. The central population consists of 9,955 star-forming, 4,567 green valley and 28,052 passive galaxies. The satellite population consists of 2,389 star-forming, 1,640 green valley and 12,080 passive galaxies.

We investigate the dependence of galaxy quenching on environment by analysing how the difference in stellar metallicity between star-forming and passive (or green valley) galaxies varies between centrals and satellites. We compute the difference in stellar metallicity between star-forming central and passive central galaxies, as well as the difference between star-forming satellite and passive satellite galaxies. As discussed earlier, the observed stellar metallicity  $\Delta Z_*$  can be used to assess the importance of starvation as a primary quenching mechanism. A larger  $\Delta Z_*$  indicates that starvation is more effective at quenching galaxies. Alternatively, a smaller  $\Delta Z_*$  may indicate that other mechanisms, such as rapid gas removal, play a more prominent role in quenching

galaxies. By comparing the observed  $\Delta Z_*$  for central galaxies and for satellite galaxies, we can assess whether starvation is more effective at quenching central or satellite galaxies, yielding insights into the role the environment plays in galaxy quenching.

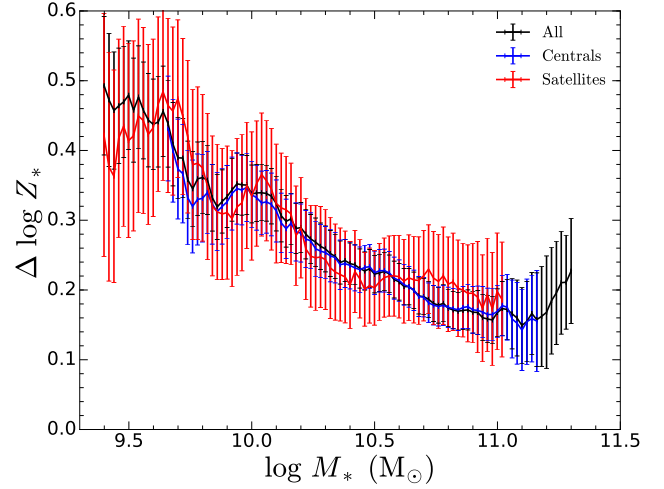
### 6.1.1 Passive galaxies (quenching at high- $z$ )

Fig. 13 shows the stellar metallicity difference between star-forming and passive galaxies, for centrals (blue), satellites (red) and the total galaxy population (centrals and satellites, black). Due to the lower statistics for satellites the data is noisier and fluctuates more considerably than the data for the central galaxies. Furthermore, the curves for the centrals and the total galaxy population are very similar because central galaxies dominate the total population. We find that the metallicity differences for central and satellite galaxies are rather consistent across the studied stellar mass range. This weak dependence of the stellar metallicity difference on the central-satellite dichotomy is consistent with the works of [Goddard et al. \(2017a\)](#) and [Zheng et al. \(2017\)](#), who analysed galaxies in the MaNGA survey on a spatially-resolved basis and found that central and satellite galaxies had very similar stellar population gradients. Since  $\Delta Z_*$  is a proxy for the effectiveness of starvation as a quenching mechanism, the lack of dependence of the stellar metallicity difference on the central-satellite dichotomy indicates that overall, the starvation mechanism operates similarly for central and satellite galaxies. This is in slight contrast with [Peng et al. \(2015\)](#), who found that satellites have slightly larger stellar metallicity enhancements compared with centrals for  $M_* < 10^{10} M_\odot$ .

We believe that this difference between our works may be due to a number of factors, which, when combined together, wash out the excess in stellar metallicity that was seen in the original work. Firstly, we use a different set of stellar metallicities in our work, derived from full spectral fitting rather than fitting spectral indices. Furthermore, we study mass-weighted stellar metallicities rather than light-weighted stellar metallicities. We also use a larger sample of galaxies together with a different approach for classifying star-forming and passive galaxies in our analysis. This will probably alter the observed stellar metallicity differences between star-forming and passive satellite/central galaxies. However, in the next section we will show that if the overdensity of galaxies is also taken into account then satellite galaxies in dense environments do show an excess of metallicity difference relative to central galaxies, indicating that the environment does have a role in some conditions, as suggested by [Peng et al. \(2015\)](#).

### 6.1.2 Green valley galaxies (quenching in the local Universe)

We now study the difference in stellar metallicity between star-forming and green valley galaxies to investigate how the quenching of green valley galaxies depends on the environment. Since local green valley galaxies have only recently started quenching, while the progenitors of local passive galaxies began quenching at much earlier epochs in cosmic history, we may expect there to be a difference in the mode



**Figure 13.** The difference in stellar metallicity between star-forming and passive galaxies, for the total galaxy population (black), the central sub-population (blue) and the satellite sub-population (red).

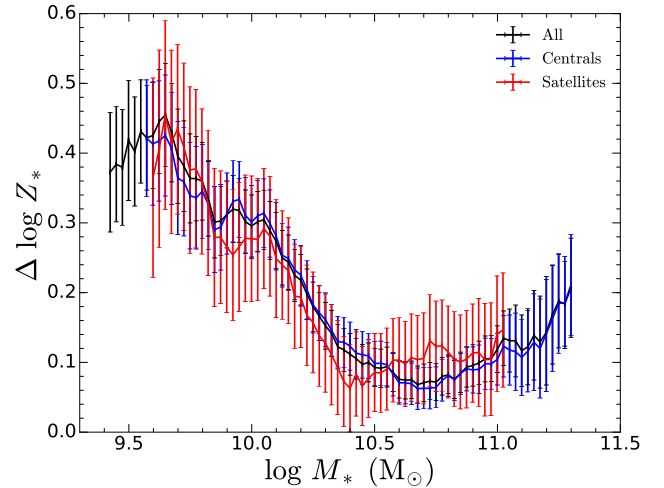


**Figure 14.** The difference in stellar metallicity between star-forming and green valley galaxies, for the total galaxy population (black), the central sub-population (blue) and the satellite sub-population (red).

responsible for quenching these two distinct populations. For example, mergers are thought to have been more effective at quenching low-mass galaxies at high-redshift, while environmental quenching could be more effective at quenching low-mass galaxies at low-redshift ([Peng et al. 2010](#)). Hence we may expect to see a stronger environmental dependence in  $\Delta Z_*$  for green valley galaxies than for passive galaxies.

We show the dependence of green valley galaxy quenching on the central-satellite dichotomy in Fig. 14. We find that, within the error of our measurements, the metallicity differences for central and satellite galaxies are consistent. Hence, as was seen in our analysis of passive galaxies, the starvation mechanism appears to operate similarly for centrals and satellites.

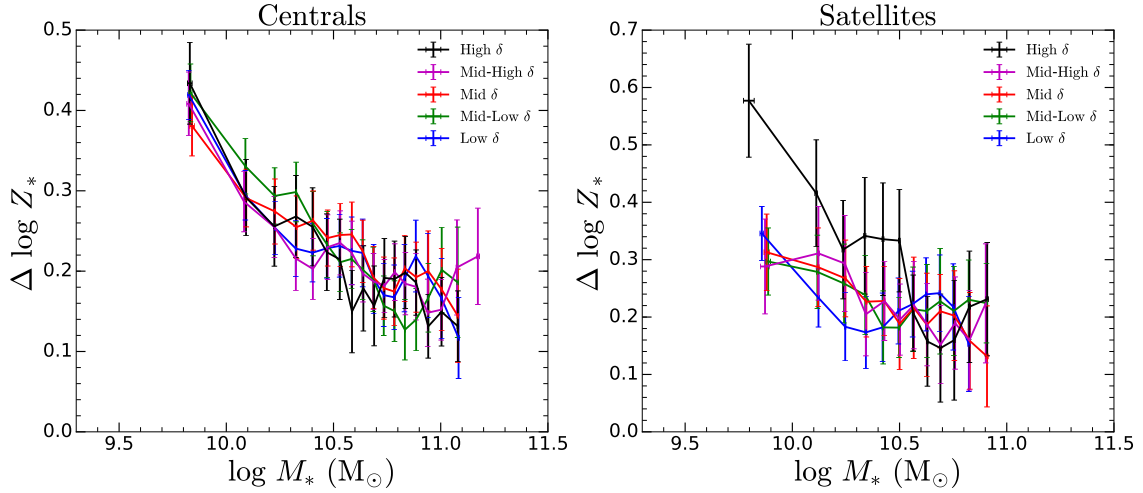


**Figure 15.** Galaxies are divided into quintiles of the local overdensity  $1 + \delta$ , ranging from the smallest (blue) to the largest overdensities (black). The stellar metallicity differences between star-forming and passive galaxies is plotted for the five overdensity quintiles as a function of  $M_*$ . Left panel: the stellar metallicity differences for central galaxies are shown. Right panel: the stellar metallicity differences for satellite galaxies are shown.

## 6.2 Local overdensity

We now focus on environmental quenching, as probed by the local overdensity. Since the local overdensity measures the relative abundance of galaxies in the local environment, it is an effective tracer of the strength and frequency of galaxy-galaxy interactions, which could potentially strip or supply gas, as well as the association of a galaxy with a group/cluster, as overdensities are obviously higher in these environments and tend to increase towards the group/cluster centre (see e.g. Peng et al. 2012), which can potentially result in a lack of cold gas accretion as galaxies plunge into the hot group/cluster halo. As with the central-satellite analysis, a dependence of  $\Delta Z_*$  on the local overdensity would indicate an environmental origin for starvation, and would make it possible to further constrain the mechanism for starvation.

We further divide the central-satellite galaxy sample into quintiles of the local overdensity. The five quintiles are defined as follows: Low (0–20th percentile), Low-Mid (20–40th percentile), Mid (40–60th percentile), Mid-High (60–80th percentile) and High (80–100th percentile). Due to the different nature of central and satellite galaxies, as well as their (potentially) central positions in galaxy groups or clusters, we have chosen to use separate overdensity quintiles for centrals and satellites. This means that the overdensity range associated with e.g. the Mid quintile for centrals will not be the same as the overdensity range associated with the Mid quintile for satellites. After dividing the sample in terms of the local overdensity, we find that the statistics in particular stellar mass regimes has become rather low. As a result, we now collect galaxies into unevenly spaced bins of stellar mass that contain an equal number of galaxies per bin. This allows us to properly assess the dependence of  $\Delta Z_*$  across a broad range of stellar mass.

### 6.2.1 Passive galaxies (quenching at high- $z$ )

We show the observed stellar metallicity difference between star-forming and passive galaxies for both centrals and satel-

lites in five different overdensity bins in Fig. 15. We find that the stellar metallicity differences for central galaxies are broadly the same across the studied local overdensity range, indicating that the quenching of central galaxies does not depend on the local overdensity, even over an overdensity range that spans 2 dex (from the Low to High quintiles). This implies that the starvation mechanism responsible for quenching central galaxies operates independently of the conditions in the local environment, indicating that internal mechanisms (i.e. mass-dependent processes) are the likely cause of starvation in central galaxies. This weak dependence of the stellar metallicity difference on the local overdensity is consistent with other works, which have also found that the local environment can have a limited influence on stellar population properties. For example, Goddard et al. (2017a) found that the stellar population gradients for central galaxies in the MaNGA survey showed no significant correlation with the local overdensity. In addition, Thomas et al. (2010) showed that the luminosity-weighted stellar ages, stellar metallicities and  $\alpha/\text{Fe}$  element ratios for local early-type galaxies did not depend on environmental density, but only depended on galaxy mass.

In addition, we find that the stellar metallicity differences for satellites are roughly consistent across most of the local overdensity range. However, we find that satellite galaxies in the highest quintile of overdensity have a significantly larger stellar metallicity enhancement compared with the satellites in environments of smaller overdensity. At  $\log(M_*/M_\odot) = 9.8$ , satellites in the High quintile typically have a  $\Delta Z_*$  that is 0.25 dex larger than satellites in the lower quintiles. This offset remains, but becomes much less significant, up to  $\log(M_*/M_\odot) = 10.5$ . So although we previously found that starvation seemingly operated independently of the central-satellite dichotomy, our more thorough analysis in terms of the local overdensity reveals that there is some signal of environmental dependence for low-mass satellite galaxies in the highest density regions. This result suggests that for the overall galaxy population, starvation operates

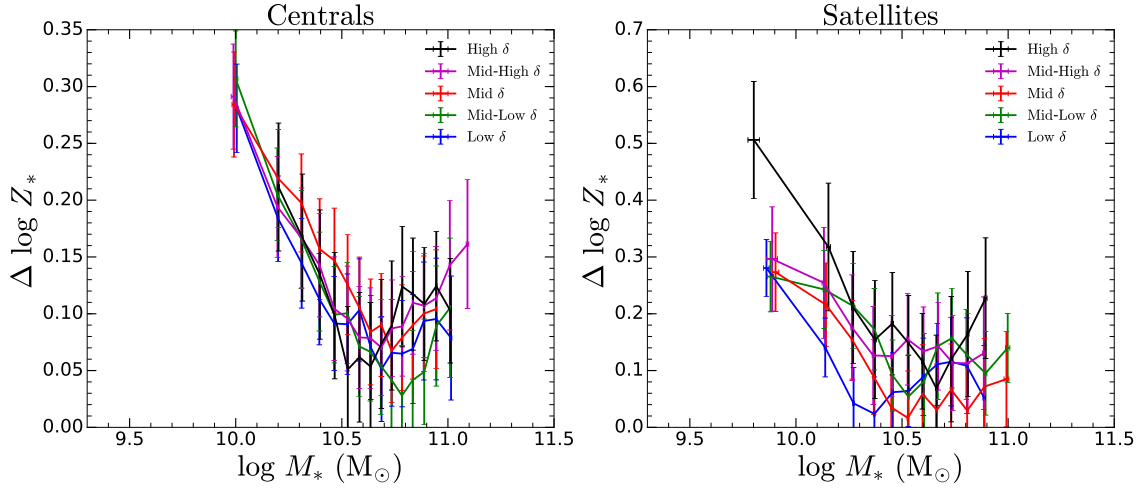


**Figure 16.** Similar to Fig. 15, but we now study the stellar metallicity difference between star-forming and green valley galaxies.

roughly independently of environment. However, for low-mass satellite galaxies in high density environments (such as clusters), environmentally-induced starvation is most effective at quenching star formation. In these systems, starvation could result from a number of physical processes, such as the removal of halo gas in galaxy-galaxy interactions and/or interruption of gas accretion as satellites plunge into the hot intracluster medium (‘strangulation’).

### 6.2.2 Green valley galaxies (quenching in the local Universe)

We also investigate how the quenching of green valley galaxies depends on the local overdensity, by studying the difference in stellar metallicity between star-forming and green valley galaxies. Our results are shown in Fig. 16. We find again that the stellar metallicity differences for central galaxies are consistent across the different overdensity regimes. Furthermore, the stellar metallicity differences for satellite galaxies are also consistent, except for low-mass satellites that are in high density environments, where we again find an excess in the stellar metallicity difference. Owing to the poorer statistics for green valley galaxies compared with passive galaxies, we find that this excess is less significant than for the passive galaxy analysis.

## 7 SUMMARY AND CONCLUSIONS

We have investigated the mechanism responsible for quenching star formation in galaxies across the cosmic epochs, i.e. the process responsible for transforming star-forming galaxies into passive systems. We leverage on the method initially developed by P15, who suggest that the stellar metallicity difference between local passive galaxies and their star-forming progenitors is a powerful tracer of the quenching process. We expand and improve upon the P15 method in the following ways:

- We adopt the spectroscopic data from SDSS DR7, which enable us to expand the statistics by a factor of two.

- We use mass-weighted stellar metallicities, which are simpler to compare with galaxy evolutionary models.
- We compare local passive galaxies with the properties of their star-forming progenitors at high redshift (in particular in terms of stellar metallicity) rather than local star-forming galaxies. We also adopt the scaling relations, in terms of gas fractions and star formation efficiency, observed for the high-redshift progenitors.

We obtain the following observational results for local passive galaxies:

- The (mass-weighted) stellar metallicity of passive galaxies is always higher than the stellar metallicity of local star-forming galaxies.
- The metallicity difference is even higher if passive galaxies are compared with their star-forming progenitors at high-redshift.
- The metallicity difference is a strong function of stellar mass, being highest at low masses and decreasing at high masses, but still remaining highly significant in the most massive galaxies analysed ( $M_* \sim 10^{11} M_\odot$ ).

By using simple analytical modelling of galaxy chemical evolution in galaxies we infer that:

- The prominent metallicity difference between passive galaxies and their star-forming progenitors implies that for galaxies at *all* masses quenching involved an extended phase of starvation, i.e. halting (or very substantial decrease) of gas accretion from the circumgalactic/intergalactic medium.
- We find that ‘effective’ outflows (i.e. outflows capable of removing gas permanently from the galaxy) are, together with starvation, of increasing importance in low-mass galaxies, with effective loading factors  $\lambda_{\text{eff}} \sim 1.5$  for galaxies with  $9.4 < \log(M_*/M_\odot) < 10$ .
- In massive galaxies ‘effective’ outflows are steadily less important; in galaxies with  $\log(M_*/M_\odot) > 11$  the effective loading factor must be lower than 0.4. This does not mean that massive galaxies are not characterised by outflows, but that most of the outflowing gas does not escape the galaxy and is being recycled. This is in line with other studies characterising outflows in massive galaxies.



- In massive galaxies ( $\log(M_*/M_\odot) \sim 11$ ) quenching started about 10 Gyr ago and the quenching phase lasted about 2 Gyr (primarily through starvation) with an  $e$ -folding time of  $\sim 1$  Gyr. This quenching time-scale is consistent with the analysis of the  $\alpha$ -elements enhancement in these systems. After 2 Gyr a sudden gas ejective/removal or heating phase must have occurred to prevent even higher chemical enrichment of the stellar population. Such delayed ejection/heating phase may have resulted from the cumulative energy of type Ia SNe, or AGN energy injection.

- In low-mass galaxies the quenching started at later cosmic epochs and the quenching time-scale was longer, up to about 6 Gyr (through a combination of starvation and outflows).

While passive galaxies have enabled us to explore the quenching mechanism at high redshift, when most of the star formation and quenching process took place, the analysis of green valley galaxies (which are currently in the transition phase between star-forming to passive) have offered us the opportunity of studying the quenching process in the local Universe. By comparing the observed stellar metallicity with simple models we infer the following:

- The significant stellar metallicity difference between green valley galaxies and local star-forming galaxies indicate that also locally the quenching process must involve an extensive period of starvation.

- The quenching time-scale appears to be longer in local galaxies, at least 3–6 Gyr (depending on mass and contribution by outflows). These are lower limits, since these galaxies are still in the transition phase and have yet to quench completely.

- Similar to high-redshift galaxies, we find that ‘effective outflows’ play an important role for local low-mass galaxies, but become gradually unimportant at high masses (implying that outflowing gas in local massive galaxies does not escape and is re-accreted).

We note however some inconsistencies between the quenching time-scale inferred from the metallicity difference between green valley and star-forming galaxies and the age difference between the two galaxy populations. There are various possible explanations for this inconsistency. One of the most important effects is that green valley galaxies are characterised by steep radial gradients in their properties (in particular age and star formation), while the SDSS DR7 single fibre captures only the central properties of these galaxies. Therefore, it is important to repeat this analysis by exploiting integral field spectroscopic galaxy surveys.

We have also investigated the metallicity difference between passive/green valley and star-forming galaxies as a function of environment. In particular we have split the sample in subsamples of central and satellite galaxies, and also in terms of galaxy overdensity. Our results can be summarised as follows:

- For most galaxies the metallicity difference between passive/green valley and star-forming does not appear to depend on galaxy overdensity or on central/satellite dichotomy.

- However, low-mass ( $\log(M_*/M_\odot) < 10$ ) satellite galaxies in the top quintile of the overdensities probed by us (i.e. close to cluster environment) are characterised by a

significantly enhanced metallicity difference between passive and star-forming and between green valley and star-forming galaxies.

- These results indicate that environmental effects contributed to the starvation of galaxies primarily in very dense environments, with effect primarily on low-mass satellite galaxies (i.e. through the process often referred to as galaxy ‘strangulation’, where accretion of cold gas is halted when low-mass galaxies plunge in the hot, dense environment of overdense regions). However, for most massive galaxies, for most central galaxies, and also for low-mass galaxies in low density environments, the starvation process must have been resulting from processes independent of environment.

We cannot constrain the mechanism responsible for starvation in the majority of galaxies for which the environment does not play a significant role. We can only speculate that one or more of the various mechanisms proposed in the literature can be at work, probably with different relative weights at different epochs and in different mass ranges. Examples of non-environmentally dependent starvation mechanisms include: heating of the galaxy halo by a radio jet; heating of the halo by quasar or star formation driven outflows, which, although may not be effective in ejective terms, can inject a significant amount of energy into the halo; gravitational shock heating.

We finally point out that the results obtained by us are correct on ‘average’, in the sense that statistically we have identified the primary quenching processes in galaxies. However, the properties of galaxies show a very large dispersion (much larger than the error on the mean shown in our figures), revealing that each individual galaxy can undergo quenching through a multitude of routes and through several different mechanisms. Only by exploiting the large statistics delivered by the Sloan Survey has it been possible to identify the underlying primary mechanisms which work, on average, for most galaxies.

## ACKNOWLEDGEMENTS

JT thanks S. Wujts for helpful discussions. JT and RM acknowledge support from the ERC Advanced Grant 695671 ‘QUENCH’. RM acknowledges support by the Science and Technology Facilities Council (STFC). YP acknowledges support from the National Key Program for Science and Technology Research and Development under grant number 2016YFA0400702, and the NSFC grant no. 11773001. Funding for the SDSS and SDSS-II has been provided by the Alfred P. Sloan Foundation, the Participating Institutions, the National Science Foundation, the U.S. Department of Energy, the National Aeronautics and Space Administration, the Japanese Monbukagakusho, the Max Planck Society, and the Higher Education Funding Council for England. The SDSS Web Site is <http://www.sdss.org/>. The SDSS is managed by the Astrophysical Research Consortium for the Participating Institutions. The Participating Institutions are the American Museum of Natural History, Astrophysical Institute Potsdam, University of Basel, University of Cambridge, Case Western Reserve University, University of Chicago, Drexel University, Fermilab, the Institute for Advanced Study, the Japan Participation Group, Johns Hopkins University, the Joint Institute for Nuclear Astrophysics,

the Kavli Institute for Particle Astrophysics and Cosmology, the Korean Scientist Group, the Chinese Academy of Sciences (LAMOST), Los Alamos National Laboratory, the Max-Planck-Institute for Astronomy (MPIA), the Max-Planck-Institute for Astrophysics (MPA), New Mexico State University, Ohio State University, University of Pittsburgh, University of Portsmouth, Princeton University, the United States Naval Observatory, and the University of Washington.

## REFERENCES

- Abadi M. G., Moore B., Bower R. G., 1999, *MNRAS*, 308, 947
- Abazajian K. N., et al., 2009, *Astrophys. J. Suppl. Ser.*, 182, 543
- Adelman-McCarthy J. K., et al., 2006, *Astrophys. J. Suppl. Ser.*, 162, 38
- Baldry I. K., Glazebrook K., Brinkmann J., Ivezić Z., Lupton R. H., Nichol R. C., Szalay A. S., 2004, *ApJ*, 600, 681
- Baldry I. K., Balogh M. L., Bower R. G., Glazebrook K., Nichol R. C., Bamford S. P., Budavari T., 2006, *MNRAS*, 373, 469
- Balogh M. L., Baldry I. K., Nichol R., Miller C., Bower R., Glazebrook K., 2004, *ApJ*, 615, L101
- Belfiore F., et al., 2017a, *MNRAS*, 170, 151
- Belfiore F., et al., 2017b, *MNRAS*, 466, 2570
- Belfiore F., et al., 2018, *MNRAS*, 477, 3014
- Birnboim Y., Dekel A., 2003, *MNRAS*, 345, 349
- Blanton M. R., et al., 2003, *ApJ*, 594, 186
- Boselli A., Cortese L., Boquien M., 2014, *A&A*, 564, A65
- Brammer G. B., et al., 2009, *ApJ*, 706, L173
- Brinchmann J., Charlot S., White S. D. M., Tremonti C., Kauffmann G., Heckman T., Brinkmann J., 2004, *MNRAS*, 351, 1151
- Chabrier G., 2003, *PASP*, 115, 763
- Chisholm J., Tremonti C. A., Leitherer C., Chen Y., 2017, *MNRAS*, 469, 4831
- Choi J., Conroy C., Moustakas J., Graves G. J., Holden B. P., Brodwin M., Brown M. J., Van Dokkum P. G., 2014, *ApJ*, 792
- Cicone C., et al., 2014, *A&A*, 562, A21
- Ciotti L., Ostriker J. P., 2007, *ApJ*, 665, 1038
- Ciotti L., Ostriker J. P., Proga D., 2009, *ApJ*, 699, 89
- Comparat J., et al., 2017, preprint, ([arXiv:1711.06575](https://arxiv.org/abs/1711.06575))
- Cortese L., Catinella B., Janowiecki S., 2017, *ApJL*, 848, L7
- Cresci G., Mannucci F., Sommariva V., Maiolino R., Marconi A., Brusa M., 2012, *MNRAS*, 421, 262
- Curti M., Cresci G., Mannucci F., Marconi A., Maiolino R., Esposito S., 2017, *MNRAS*, 465, 1384
- Daddi E., et al., 2007, *ApJ*, 670, 156
- Dekel A., Birnboim Y., 2006, *MNRAS*, 368, 2
- Dekel A., Silk J., 1986, *ApJ*, 303, 39
- Doi M., et al., 2010, *AJ*, 139, 1628
- Dressler A., 1980, *ApJ*, 236, 351
- Eisenstein D. J., Annis J., Gunn J. E., Szalay A. S., Connolly A. J., 2001, *AJ*, 122, 2267
- Elbaz D., et al., 2007, *A&A*, 468, 33
- Erb D., Shapley A., Pettini M., 2006, *ApJ*, 644, 813
- Fabian A. C., 2012, *ARA&A*, 50, 455
- Farouki R., Shapiro S. L., 1981, *ApJ*, 243, 32
- Finlator K., Dave R., 2008, *MNRAS*, 385, 2181
- Fluetsch A., et al., 2018, preprint, ([arXiv:1805.05352](https://arxiv.org/abs/1805.05352))
- Fossati M., et al., 2017, *ApJ*, 835
- Gallazzi A., Charlot S., Brinchmann J., White S. D. M., Tremonti C. A., 2005, *MNRAS*, 362, 41
- Gallazzi A., Brinchmann J., Charlot S., White S. D. M., 2008, *MNRAS*, 383, 1439
- Gallazzi A., Bell E. F., Zibetti S., Brinchmann J., Kelson D. D., 2014, *ApJ*, 788, 72
- Genzel R., et al., 2015, *ApJ*, 800, 20
- Goddard D., et al., 2017a, *MNRAS*, 465, 688
- Goddard D., et al., 2017b, *MNRAS*, 466, 4731
- González Delgado R. M., et al., 2014, *ApJL*, 791
- Gunn J. E., Gott, J. Richard I., 1972, *ApJ*, 176, 1
- Gunn J., Carr M., Rockosi C., Sekiguchi M., 1998, *AJ*, 116, 67
- Gunn J. E., et al., 2006, *AJ*, 131, 2332
- Guo Y., et al., 2017, *ApJL*, 841, 8
- Halliday C., et al., 2008, *A&A*, 479, 417
- Heckman T. M., Alexandroff R. M., Borthakur S., Overzier R., Leitherer C., 2015, *ApJ*, 809, 147
- Kauffmann G., et al., 2003, *MNRAS*, 341, 33
- Kennicutt R. C., 1998, *ApJ*, 498, 541
- Kereš D., Katz N., Weinberg D. H., Davé R., 2005, *MNRAS*, 363, 2
- King A., Pounds K., 2015, *ARA&A*, 53, 115
- Kovač K., et al., 2010, *ApJ*, 708, 505
- Kroupa P., 2001, *MNRAS*, 322, 231
- Kuntschner H., Smith R. J., Colless M., Davies R. L., Kaldare R., Vazdekis A., 2002, *MNRAS*, 337, 172
- Lara-López M. A., et al., 2010, *A&A*, 521, L53
- Larson R. B., 1974, *MNRAS*, 169, 229
- Larson R. B., Tinsley B. M., Caldwell C. N., 1980, *ApJ*, 237, 692
- Lian J., Thomas D., Maraston C., Goddard D., Comparat J., Gonzalez-Perez V., Ventura P., 2018a, *MNRAS*, 474, 1143
- Lian J., et al., 2018b, *MNRAS*, 476, 3883
- Lian J., Thomas D., Maraston C., 2018c, preprint, ([arXiv:1809.04079](https://arxiv.org/abs/1809.04079))
- Lonoce I., et al., 2015, *MNRAS*, 454, 3912
- Maiolino R., et al., 2008, *A&A*, 488, 463
- Mannucci F., et al., 2009, *MNRAS*, 398, 1915
- Mannucci F., Cresci G., Maiolino R., Marconi A., Gnerucci A., 2010, *MNRAS*, 408, 2115
- Maraston C., Strömbäck G., 2011, *MNRAS*, 418, 2785
- Matteucci F., Panagia N., Pipino A., Mannucci F., Recchi S., Della Valle M., 2006, *MNRAS*, 372, 265
- Mcgee S. L., Balogh M. L., Wilman D. J., Bower R. G., Mulchaey J. S., Parker L. C., Oemler A., 2011, *MNRAS*, 413, 996
- Moore B., Katz N., Lake G., Dressler A., Oemler A. J., 1996, *Nature*, 379, 613
- Murray N., Quataert E., Thompson T. A., 2005, *ApJ*, 618, 569
- Muzzin A., et al., 2013, *ApJ*, 777, 18
- Muzzin A., et al., 2014, *ApJ*, 796
- Noeske K. G., et al., 2007, *ApJ*, 660, 43
- Onodera M., et al., 2015, *ApJ*, 808, 161
- Panther B., Jimenez R., Heavens A. F., Charlot S., 2008, *MNRAS*, 391, 1117
- Peng Y. J., Maiolino R., 2014a, *MNRAS*, 438, 262
- Peng Y. J., Maiolino R., 2014b, *MNRAS*, 443, 3643
- Peng Y.-j., et al., 2010, *ApJ*, 721, 193
- Peng Y.-j., Lilly S. J., Renzini A., Carollo M., 2012, *ApJ*, 757, 23
- Peng Y., Maiolino R., Cochrane R., 2015, *Nature*, 521, 192
- Petrosian V., 1976, *ApJ*, 209, L1
- Pipino A., Matteucci F., 2004, *MNRAS*, 347, 968
- Pipino A., Matteucci F., 2006, *ApJ*, 638, 739
- Pipino A., Ercole A. D., Matteucci F., 2008, *A&A*, 484, 679
- Pipino A., Lilly S. J., Carollo C. M., 2014, *MNRAS*, 441, 1444
- Popping G., Somerville R. S., Trager S. C., 2014, *MNRAS*, 442, 2398
- Prochaska J. X., Wolfe A. M., 2009, *ApJ*, 696, 1543
- Ranalli P., Comastri A., Origlia L., Maiolino R., 2008, *MNRAS*, 386, 1464
- Reddy N. A., Pettini M., Steidel C. C., Shapley A. E., Erb D. K., Law D. R., 2012, *ApJ*, 754
- Renzini A., Peng Y.-j., 2015, *ApJ*, 801, L29

- Rhee J., Lah P., Chengalur J. N., Briggs F. H., Colless M., 2016, *MNRAS*, 460, 2675
- Salim S., et al., 2007, *Astrophys. J. Suppl. Ser.*, 173, 267
- Salpeter E. E., 1955, *ApJ*, 121, 161
- Sanchez-Blazquez P., et al., 2006, *MNRAS*, 371, 703
- Santini P., et al., 2014, *A&A*, 562, A30
- Schinnerer E., et al., 2016, *ApJ*, 833, 112
- Schmidt M., 1959, *ApJ*, 129, 243
- Scoville N., et al., 2017, *ApJ*, 837, 150
- Sklias P., Schaerer D., Elbaz D., Pannella M., Schreiber C., Cava A., 2017, *A&A*, 605, A149
- Smee S. A., et al., 2013, *AJ*, 146
- Sommariva V., Mannucci F., Cresci G., Maiolino R., Marconi A., Nagao T., Baroni A., Grazian A., 2012, *A&A*, 539, A136
- Spitoni E., Vincenzo F., Matteucci F., 2017, *A&A*, 599, A6
- Strateva I., et al., 2001, *AJ*, 122, 1861
- Strauss M. A., et al., 2002, *AJ*, 124, 1810
- Tacconi L. J., et al., 2013, *ApJ*, 768, 74
- Tacconi L. J., et al., 2018, *ApJ*, 853, 1
- Terlevich A. I., Forbes D. A., 2002, *MNRAS*, 330, 547
- Thomas D., Maraston C., Bender R., 2005, *ApJ*, 621, 673
- Thomas D., Maraston C., Schawinski K., Sarzi M., Silk J., 2010, *MNRAS*, 404, 1775
- Tinsley B. M., 1980, *Fundamentals Cosmic Phys.*, 5, 287
- Tremonti C. A., et al., 2004, *ApJ*, 613, 898
- Van Den Bosch F. C., Aquino D., Yang X., Mo H. J., Pasquali A., McIntosh D. H., Weinmann S. M., Kang X., 2008, *MNRAS*, 387, 79
- Vincenzo F., Matteucci F., Belfiore F., Maiolino R., 2016a, *MNRAS*, 455, 4183
- Vincenzo F., Belfiore F., Maiolino R., Matteucci F., Ventura P., 2016b, *MNRAS*, 458, 3466
- Wetzel A. R., Tinker J. L., Conroy C., 2012, *MNRAS*, 424, 232
- Wetzel A. R., Tinker J. L., Conroy C., van den Bosch F. C., 2013, *MNRAS*, 432, 336
- Wilkinson D. M., Maraston C., Goddard D., Thomas D., Parikh T., 2017, *MNRAS*, 472, 4297
- Wuyts S., et al., 2011, *ApJ*, 742, 20
- Yang X., Mo H. J., Van Den Bosch F. C., Jing Y. P., 2005, *MNRAS*, 356, 1293
- Yang X., Mo H. J., van den Bosch F. C., Pasquali A., Li C., Barden M., 2007, *ApJ*, 671, 153
- York D. G., et al., 2000, *AJ*, 120, 1579
- Zheng Z., et al., 2017, *MNRAS*, 465, 4572
- van der Wel A., et al., 2014, *ApJ*, 788, 19

## APPENDIX A: MOLECULAR GAS RELATIONS

We used the integrated Schmidt-Kennicutt (SK) law, given by equation (3), to parametrize star formation in our models. The total gas mass, which includes both the atomic and molecular components, as well as the total gas depletion time were used in the SK law in the main body of the paper. In this section, we investigate how our model predictions and conclusions change when only the molecular gas component is considered. In this case, the law for star formation becomes

$$\Psi = \epsilon_m \dot{m}, \quad (\text{A1})$$

where  $\epsilon_m$  is the star formation efficiency for molecular gas and  $\dot{m}$  is the molecular gas mass.  $\epsilon_m$  is related to  $t_{\text{depl},m}$ , the molecular gas depletion time, through  $\epsilon_m = 1/t_{\text{depl},m}$ .

There are two main differences between models that use the total gas mass and models that only use the molecular component. Firstly, molecular gas reservoirs are smaller

than the total gas reservoirs. Hence outflows with a given outflow rate  $\Lambda$  will be more effective at quenching star formation in models that only contain molecular gas. This means that leaky-box models that only contain molecular gas will have more difficulty in reproducing the large stellar metallicity differences that have been observed. As a result, these models will tend to disfavour quenching through outflows. Secondly, molecular gas depletion time-scales are shorter than total gas depletion time-scales. Models that only contain molecular gas will process and enrich the gas in the ISM more rapidly. As a result, the stellar metallicity increases more quickly and so the quenching time-scales derived from our analysis of stellar metallicity differences tend to be shorter. These differences between the total gas and molecular gas models are most apparent for low-mass galaxies, as these tend to have relatively larger atomic-to-molecular gas mass ratios than the more massive galaxies. The model predictions for low-mass galaxies are therefore more strongly affected by the removal of the atomic gas component.

### A1 Passive galaxies

We compare the observed stellar metallicity differences between star-forming and passive galaxies with the predictions from gas regulator models that only contain molecular gas. Our results using a closed-box model with  $\lambda_{\text{eff}} = 0$  is shown in Fig. A1. We find that our models are able to reproduce the observations, and the derived quenching time-scales are shorter than what was seen in Fig. 6. We also show the predictions using a leaky-box model with  $\lambda_{\text{eff}} = 1$  in Fig. A2. In this case our models struggle to reproduce the observed stellar metallicity differences, which suggests that outflows played a minor role in quenching the progenitors of passive galaxies.

### A2 Green valley galaxies

We now study the stellar metallicity differences between star-forming and green valley galaxies. Our results for the closed-box model are shown in Fig. A3. The quenching time-scales are typically 3 Gyr and are shorter than what was seen in Fig. 10. The predictions from the leaky-box model with  $\lambda_{\text{eff}} = 1$  are shown in Fig. A4. We find that models invoking outflows are unable to reproduce the observed stellar metallicity differences, suggesting that outflows do not play a significant role in quenching star formation in local galaxies.

This paper has been typeset from a  $\text{\TeX}/\text{\LaTeX}$  file prepared by the author.

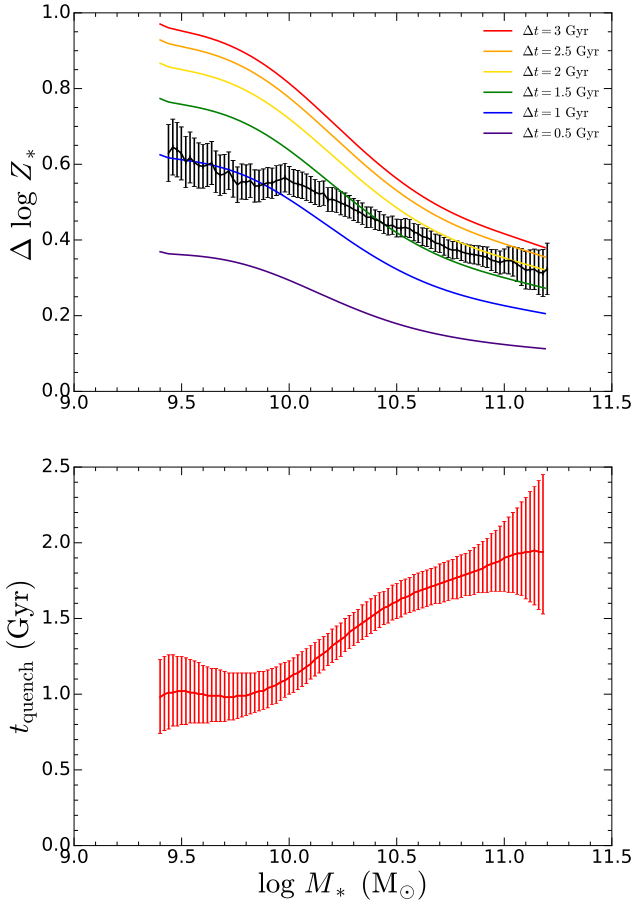


**Figure A1.** Similar to Fig. 6, where we study the stellar metallicity differences between star-forming and passive galaxies using a closed-box model with  $\lambda_{\text{eff}} = 0$ , but now we only use the molecular gas component in our models.

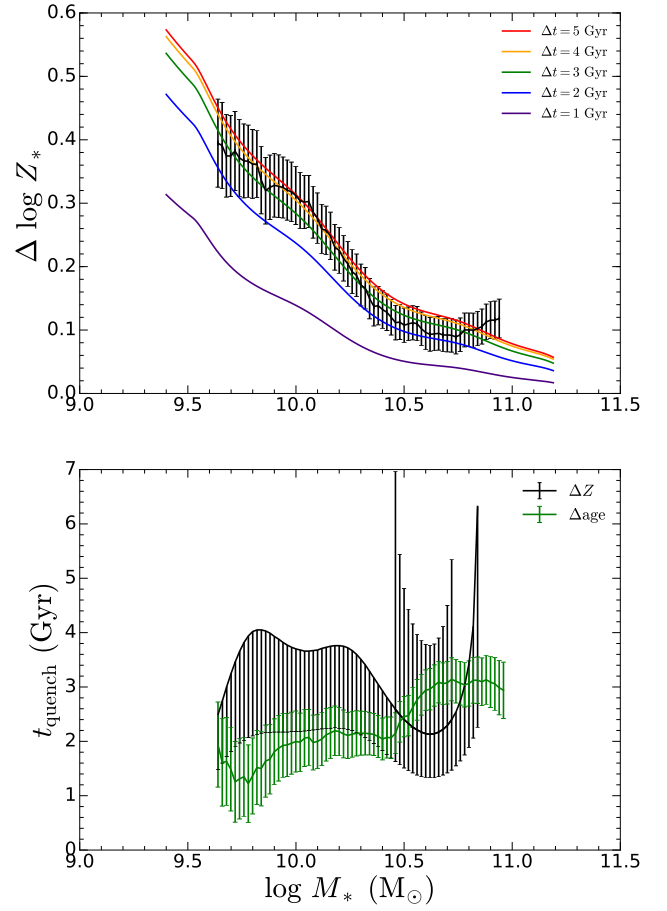


**Figure A3.** Similar to Fig. 10, where we study the stellar metallicity differences between star-forming and green valley galaxies using a closed-box model with  $\lambda_{\text{eff}} = 0$ , but now we only use the molecular gas component in our models. In the cases when the upper limit on the stellar metallicity difference  $\Delta Z_*$  cannot be reproduced by our model, only the lower limit on the quenching time-scale  $t_{\text{quench}}$  is shown.

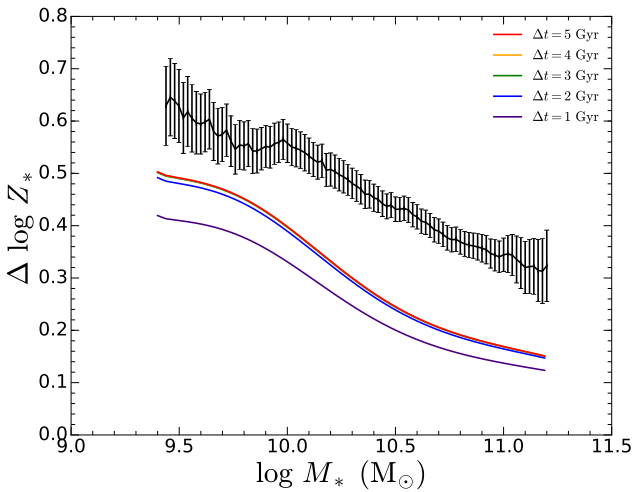


**Figure A2.** Similar to Fig. A1, but we now consider a leaky-box model, incorporating outflows with  $\lambda_{\text{eff}} = 1$ .

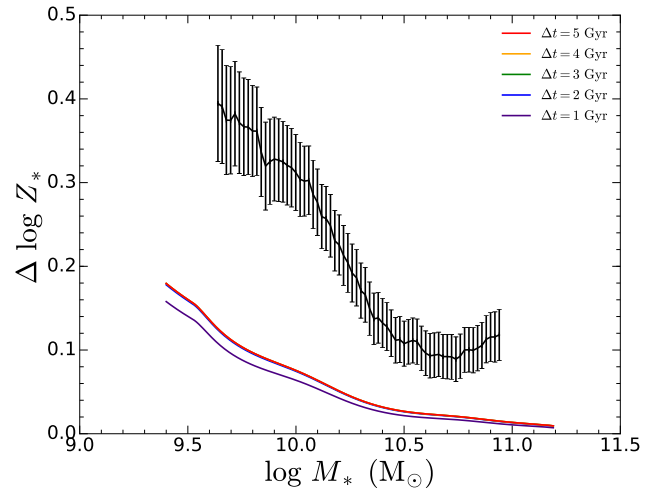


**Figure A4.** Similar to Fig. A3, but we now consider a leaky-box model, incorporating outflows with  $\lambda_{\text{eff}} = 1$ .